R. & M. No. 3033
(16,528)
A.R.C. Technical Report

MINISTRY OF SUPPLY

AERONAUTICAL RESEARCH COUNCIL
REPORTS AND MEMORANDA

A Survey and Correlation of Data on Heat Transfer by Forced Convection at Supersonic Speeds

By

R. J. MONAGHAN, M.A.

LONDON: HER MAJESTY'S STATIONERY OFFICE
1958
FIFTEEN SHILLINGS NET

A Survey and Correlation of Data on Heat Transfer by Forced Convection at Supersonic Speeds

By

R. J. MONAGHAN, M.A.

COMMUNICATED BY THE DIRECTOR-GENERAL OF SCIENTIFIC RESEARCH (AIR), MINISTRY OF SUPPLY

Reports and Memoranda No. 3033*

September, 1953

Summary.—This report surveys and, wherever possible, correlates experimental data available in the United Kingdom up to January 1953 on heat transfer by forced convection to bodies moving through the air at supersonic speeds (or the corresponding wind-tunnel problem). The main aim of the investigation was to seek possible explanations for the occasional apparent inconsistencies between wind-tunnel results from different sources, between wind-tunnel and flight results and between either type of experimental results and the predictions of theory.

The main topics covered are kinetic temperature rise, heat-transfer coefficients and transition from laminar to turbulent flow.

Conclusions are reached concerning the reliability of the data for design purposes and suggestions are made concerning the most useful fields of study for future experimental work.

Additional note to Summary. October, 1956.

A considerable amount of further evidence has become available in the years since 1953 and in places it is necessary to amend some of the statements made in this report. This has been done by adding footnotes prefixed by the date 1956.

1. *Introduction.*—The field of heat transfer by forced convection to bodies moving at high speeds has received an increasing amount of attention in recent years and from the designer's point of view there is a growing problem of how accurately he can expect data obtained mainly in wind tunnels to forecast the skin temperatures likely to be attained in flight. The problem is complicated by occasional apparent inconsistencies between wind-tunnel results from different sources, between wind-tunnel results and the few available flight results and last but not least between either type of experimental result and the predictions of theory.

The above problems form the basis of the present survey. To keep it down to reasonable physical dimensions consideration is given, as stated above, only to the case of bodies moving at supersonic speeds in air (or the corresponding wind-tunnel problem), which is only a portion of the general problem of heat transfer in compressible flow. Also it does not include the problems of slip, or of free-molecule flow, which are encountered at very high altitudes.

The majority of the reports considered were issued in the years 1949 to 1952. A survey of earlier literature has already been made by Johnson and Rubesin[1] and the United States Air Force has issued a comprehensive bibliography[2] covering the same period.

* R.A.E. Tech. Note Aero. 2259, received 3rd February, 1954.

More recently, Rubesin, Rumsey and Varga[3] and Gazley[4] have made reviews which cover some of the same ground as the present survey, but with differences at times either in detail, or in emphasis, or in interpretation. These reviews[3,4] should be read in conjunction with the present note.

In preparing the survey, the aim was to produce as clear and as self-contained a physical picture as possible of the present state of knowledge, separating as much as possible the effects of individual parameters which invariably appear in various combinations during either wind-tunnel or flight tests.

To keep the main discussion reasonably connected, the various symbols and coefficients are defined in section 2, which gives a brief non-rigorous account of the factors influencing heat transfer by forced convection in high-speed flow. This section also provides the framework around which the remainder of the note is built and in the subsequent sections the various items are considered separately and their experimental values are presented and discussed. Major emphasis is placed on flight-test data when available and reasons are sought to explain any discrepancies between them and wind-tunnel or theoretical results.

2. *Conditions Affecting Heat Transfer.*—Suppose a body is moving steadily with velocity u_∞ through a gas of density ρ_∞ and temperature T_∞ (ambient density and ambient temperature, the latter in degrees absolute). Then relative to the body, conditions are as shown in Fig. 1 and T_∞ is now the static temperature of the approaching stream (ahead of the bow shock wave if the speed is supersonic). From the principle of the conservation of energy, the total (or stagnation) temperature $T_{H\infty}$ of this stream is:

$$T_{H\infty} = T_\infty + u_\infty^2/2Jc_p \qquad \ldots \quad \ldots \quad \ldots \quad \ldots \quad \ldots \qquad (1)$$

where c_p is the specific heat of the gas at constant pressure, assumed constant*

and J is the mechanical equivalent of heat.

The Mach number of the approaching stream is M_∞ $(= u_\infty/a_\infty)$ and it will be referred to as the 'free-stream Mach number'.

The presence of the body will disturb the flow and we shall denote conditions along a streamline in its neighbourhood (behind the bow shock wave) by subscript $_1$. The total temperature of the gas following such a streamline is then T_{H1} and if no energy has been added or subtracted we have:

$$T_{H1} = T_{H\infty} . \qquad \ldots \quad \ldots \quad \ldots \quad \ldots \quad \ldots \qquad (2)$$

If the gas were an ideal fluid and no heat was being exchanged between it and the body (zero heat-transfer conditions), then equation (2) would apply to all streamlines right in to the surface of the body. In practice, energy can be transferred across the streamlines by the effects of

---

* For air c_p is within 2 per cent of a constant value for temperatures up to the order of 200 deg C. The effect of its variation at higher temperatures is included in the graphs of Ref. 45.

Also in equation (1) and throughout the survey it is assumed that the various quantities are expressed in consistent units. These are given in the list of symbols on the basis of slugs, feet, seconds as the units of mass, length and time. One slug is taken as g_0 lb mass, where g_0 is the numerical value of the acceleration due to gravity under standard conditions. For the majority of practical purposes this gives the unit of force as one lb weight.

The units of temperature and heat are taken as degrees centigrade and C.H.U. (centigrade heat units).

This differs from the convention adopted in Ref. 45, where the most commonly quoted values were used in each instance, which led to the insertion of a factor g in equations such as equation (1) above.

viscosity and thermal conductivity, but, except at very low speeds or in a very rarefied atmosphere, these effects are confined to limited regions close to the body known as 'boundary layers'. Outside these boundary layers equation (2) applies and in future we shall take subscript $_1$ as denoting conditions in the stream outside the boundary layer. The Mach number of this stream is M_1 and it will be referred to as the 'local Mach number'.

For simplicity, only a nose cone (of apex angle θ) of a body has been shown in Fig. 1 and the local conditions are constant along its length. In general, however, the local conditions may vary along the length of the body.

Turning now to the boundary layers, there are two. There is a velocity boundary layer wherein the effects of viscosity (tangential stresses) are of importance and its dimensions and behaviour are linked with Reynolds number R or $Re = \rho ux/\mu$ (ratio of inertia forces to viscous forces).

Where ρ is density

μ is viscosity

and x is a typical linear dimension.

There is also a thermal boundary layer wherein the effects of thermal conductivity (heat transfer by conduction) are of importance and it is linked with Peclet number $Pe = \rho c_p ux/k$ (ratio of heat transfer by forced convection to heat transfer by conduction), where k is thermal conductivity.

It is only when Re and Pe are large that the boundary-layer approximation described above applies. In general, the larger they are, the thinner the boundary layers become.

A link between the two boundary layers is useful. This is provided by taking the ratio of Peclet number to Reynolds number, *i.e.*, $Pe/Re = c_p\mu/k$, and this is Prandtl number, which we shall denote by σ. Note that Prandtl number depends only on the physical properties of the gas. For air, σ is of the order of $0 \cdot 7$ (*see* Ref. 6), and we might expect a close relation between the two boundary layers. For example the ratio of the thicknesses (δ) is approximately given theoretically by $\delta_T/\delta_u \doteq \sigma^{-1/3}$, $\doteq 1 \cdot 13$ for air, so that experimentally it would be very difficult to assign separate values to δ_T and δ_u for air. In future then we shall talk in terms of a single boundary layer, characterised by Reynolds number and we may expect that any relations between the effects of viscosity (*e.g.*, skin friction) and thermal conductivity (*e.g.*, heat transfer) will involve Prandtl number. In the above it is assumed that the temperature is uniform over the length of the body so that Re and Pe are based on the same linear dimension.

The above discussion applies to streamline or laminar flow as is obtained over the forward portion of the body. Further back there is transition to turbulent or eddying flow in the boundary layer and throughout most of it the eddies take control of the transfer of momentum and energy normal to the surface. However, the effects in the boundary layer can still be related to Reynolds number and since the 'effective Prandtl number' of the eddying flow appears to be close to unity, there is still no confusion in thinking in terms of a single boundary layer.

Transition is imperfectly understood, but it takes place over a finite length instead of at a discrete point as shown in Fig. 1. However, it is more convenient for the purposes of analysis to assume a transition point instead of region and the results of Refs. 9 and 10 indicate that this point should be taken at the beginning of the transition region*. Aft of the transition point the flow is assumed to be fully turbulent.

* There is now (1956) more knowledge concerning the mechanism of transition, *e.g.*, *see* Ref. 61, and it would be more correct to say that the transition 'point' fluctuates with time over a finite distance. Time-averaging instrumentation, such as a pitot-tube, will indicate a transition 'region' and the present trend is to take the transition 'point' to occur at the end (not at the beginning) of this region.

We can now return to consideration of the temperature conditions within the boundary layer. Provided the thickness of the boundary layer is great* compared with the mean free path of the molecules of air, *i.e.*, provided we are operating under continuum flow conditions, then the air in contact with the surface of the body is at rest. Therefore under zero heat-transfer conditions, if equations (1) and (2) were applicable, the temperature of the surface would be T_{H1}. However, in general the conflicting actions of viscosity and thermal conductivity cause a re-distribution of energy across the boundary layer and the surface temperature for zero heat transfer (T_{w0}) is unequal to the free-stream total temperature T_{H1}. In general if:

$$\sigma \gtreqless 1 \text{ then } T_{w0} \gtreqless T_{H1} .$$

For air, σ is less than unity and therefore conditions are as shown in Fig. 1. It is convenient to define a temperature recovery factor β by:

$$\beta = \frac{T_{w0} - T_1}{T_{H1} - T_1} \quad \ldots \quad (3)$$

and it may be noted that β may take different values depending on whether the boundary layer is laminar or turbulent. ($T_{w0} - T_1$) is known as the 'kinetic temperature rise'.

If heat is being transferred between the body and the air stream (in either direction) then although its thickness may be altered, the gain or loss of heat is apparent only in the boundary layer, and passes downstream from the body into the wake. Outside this region equation (2) is still applicable.

Heat is transferred by radiation, and by conduction at the body–air interface, the latter being governed by the forced convection in the boundary layer. Considering the conduction–convection problem, we can define a heat-transfer coefficient h by:

$$h = \frac{q}{\Delta T}, \quad \ldots \quad (4)$$

where q is the heat transferred per unit time per unit area

and ΔT is a representative temperature difference between body and fluid.

Equation (4) is an expression of Newton's cooling law, but except over a limited range h is by no means independent of temperature as was originally assumed. A more useful heat-transfer coefficient is given by:

$$k_H = \frac{h}{\rho u c_p}, \quad \ldots \quad (5)$$

which can be related directly to skin-friction coefficient *via* a function of Prandtl number and shows the same variation with Reynolds number†.

* The usual criterion for this is $\sqrt{(Re/M)} > 100$. Lesser values indicate that we are in the slip flow region, but it is possible that the results of the present note may be applied without serious error down to $\sqrt{(Re/M)} > 10$.

† k_H is also known as the Stanton number, St. Another coefficient in general use is Nusselt number $N_u = hx/k$ which, however, suffers from the disadvantage that it cannot be correlated on the same plot as skin-friction coefficient. It can easily be verified that $k_H = N_u/\sigma Re$.

The physical significance of k_H is that it represents the ratio of the heat supplied (or abstracted) per unit area to the heat that would be required to raise (or lower) the temperature of a unit cross-section of the flowing air by ΔT in unit length of travel. k_H decreases with increase of Reynolds number and for a given Reynolds number is larger for a turbulent than for a laminar boundary layer. It is usual to set $u = u_1$ and the question of the best temperature at which to evaluate the physical properties of air both in k_H and in Re is considered in the appropriate sections of this note. (Except near a flow separation from the body, the static pressure is constant across the boundary layer, so that from the equation of state $p = \rho \bar{R} T$ where $\bar{R}$ is the gas constant, there is an inverse relation between density and temperature).

There remains the question of the representative temperature difference ΔT. Intuition, theory[20] and experiment all support the choice of:

$$\Delta T = T_{w0} - T_w \quad \ldots \quad (6)$$

where T_{w0} is the surface temperature for zero heat transfer

and T_w is the actual local surface temperature (*see* Fig. 1).

(There are theoretical indications[23] that modifications may become necessary at high Mach numbers). Accepting equation (6), we can re-write equation (4) as:

$$h = \frac{q}{T_{w0} - T_w}. \quad \ldots \quad (7)$$

Thus if T_w is less than T_{w0}, heat will flow from the air into the body and this is known as 'aerodynamic heating'.

As regards heat transfer by radiation, the major items are (*a*) radiation away from the body to its surroundings and (*b*) the influx to the body of solar radiation. These are discussed in Ref. 45. In flight the surface will reach an equilibrium temperature when the heat inflow by aerodynamic heating and solar radiation is balanced by the heat loss by radiation away from the surface. The amount by which this equilibrium temperature differs from the zero heat-transfer temperature depends on numerous factors, among them being speed, height, surface condition and state of boundary layer. Once again *see* Ref. 45 for a more complete discussion.

Finally it should be mentioned that theory and the majority of wind-tunnel results are for steady flow conditions, whereas in flight the interest may be in accelerating or decelerating flow conditions. The question as to the validity of applying data obtained in the former to estimate skin temperatures appropriate to the latter is answered to some extent by the correlations obtained later in this note.

3. *Kinetic Temperature Rise.*—3.1. *Flat Plates and Bodies of Revolution with Axes in Stream Direction.*—In these cases we consider the non-dimensional local-temperature recovery factor:

$$\beta = \frac{T_{w0} - T_1}{T_{H1} - T_1}, \quad \ldots \quad (3)$$

which represents an attempt to eliminate the Mach-number effect apparent in the kinetic temperature rise $(T_{w0} - T_1)$.

Theoretically and by imposing certain restrictions including constancy of Prandtl number on the thermal properties of the fluid, Crocco[20] has shown that for a laminar boundary layer on a flat plate in compressible flow:

$$\beta \simeq \sigma^{1/2}, \quad \ldots \quad (8)$$

which is the same result as obtained by Pohlhausen for isothermal flow (*e.g.*, Ref. 21). For the turbulent boundary layer in isothermal flow Squire[22] has suggested the formula:

$$\beta = \sigma^{(n+1)/(n+3)} , \qquad \ldots \qquad (9a)$$

where n is the index in the power-law velocity distribution $(u/u_1) = (y/\delta)^n$.

For $n \leqslant 1/7$ and values of σ near unity it is sufficiently accurate to take:

$$\beta = \sigma^{1/3} . \qquad \ldots \qquad (9b)$$

Experimentally it is very difficult to obtain zero heat-transfer conditions. In a conventional supersonic wind tunnel the aerodynamic heat-transfer rates are small because of the reduced density, so that stray conduction through the model supports to the outside air and thermal lags due to the heat capacity of the model may make it appear that zero heat-transfer temperature conditions have been reached when in fact heat is still being transferred (*e.g.*, Ref. 10). In flight the same difficulties may repeat themselves because of radiation effects and in both cases there is the difficulty that temperature gradients along the body may alter the local zero heat-transfer conditions (*see* section 5.2.1. below).

3.1.1. *Wind-tunnel results*.—For the above reasons the wind-tunnel results in Figs. 2 and 3 have been divided arbitrarily into:

(*a*) those from continuous-flow tunnels, where there was the opportunity to stabilise temperatures (Fig. 2)

(*b*) those from intermittent-flow tunnels where some extrapolation or pre-setting of temperatures may have been necessary (Fig. 3).

3.1.1.1. *Results from continuous-flow tunnels* (*Fig.* 2).—Considering Fig. 2 we see that for laminar boundary layers the results for bodies of revolution (Fig. 2b) are reasonably close to the theoretical value of $\sigma^{1/2} = 0 \cdot 848$ (for $\sigma = 0 \cdot 72$), whereas for flat plates (Fig. 2a) the recovery factor is about $0 \cdot 88$. This may be linked with the fact that the measured laminar boundary layer on a cone[17] agrees quite well with theory, whereas that on a flat plate appears to suffer from a leading-edge disturbance (*e.g.*, Ref. 10) and yields over-large values for rate of growth, etc., as estimated from pitot traverse measurements*.

It should be mentioned that the flat-plate results at the two lowest Reynolds numbers obtained by Monaghan and Cooke[10] at $M = 2 \cdot 82$ (Fig. 2a) were for a laminar boundary layer, but are slightly higher than the subsequent turbulent recovery factors. The same effect was found by Hilton[13] in his experiments on a tangent-ogive (Fig. 2b), but the majority of the results in Fig. 2 indicate that the laminar recovery factor is less than the turbulent and the more nearly the layer is truly laminar the more nearly the recovery factor approaches the value $\sigma^{1/2}$ of equation 8.

Turning to the turbulent boundary layer, the recovery factors for both flat plates and bodies of revolution in Fig. 2 lie near to the value $\sigma^{1/3}$ (for $\sigma = 0 \cdot 72$). The values for bodies of revolution are slightly lower than those for flat plates, but of more importance is the fact that both sets of results show a tendency towards a decrease in recovery factor with increase in Reynolds number. This is the opposite effect to that which would have been expected from equation (9*a*) and low-speed flow measurements of velocity profile, where increase in Reynolds number results in a decrease in the index n (*e.g.*, Ref. 21), and hence an increase in recovery factor would be expected.

---

* (1956). Conduction within the plate from under surface to upper surface in the leading-edge region may be the dominant cause of these high recovery factors.

3.1.1.2. *Results from intermittent-flow tunnels* (*Fig.* 3).—A peculiarity of the results shown in Fig. 3 is the very high recovery factors found by Fallis[19] for a flat plate and by Eber[16] for a body of revolution, both in the region of one million Reynolds number. Both authors attribute the high values to the fact that the boundary layer may be in the transition region between laminar and turbulent flow. (In this respect it may be noted that Slack[41] obtained a similar result for a flat plate in a continuous-flow tunnel. In his case recovery factors were estimated by extrapolation to zero of measured heat-transfer rates and for that reason they were not included in Fig. 2).

As a check on Eber's results, Stine and Scherrer[14] tested a similar model of a cone-cylinder both in a continuous-flow and in an intermittent-flow tunnel. The results from both tunnels were in agreement and, as Fig. 3b shows, lie in the regions already found from the continuous-flow tunnel results of Fig. 2, there being a smooth transition between the laminar and turbulent boundary-layer values. Stine and Scherrer[14] suggest that the discrepancy between Eber's results[16] and their own may be caused by 'possible differences in the conditions which caused transition' (*e.g.*, tunnel turbulence level).

There is also the difficulty mentioned at the beginning of this section that the time of blow in an intermittent tunnel may be too short for accurate measurement of the zero heat-transfer condition. In the tunnel used by Fallis[19] the blowing time was about 25 seconds and considerable extrapolation of curves of skin temperature against time was necessary. The blowing time during Eber's tests[16] is not stated, but in the case of Stine and Scherrer[14] it varied between 18 minutes at $M_0 = 2$, and 5 minutes at $M_0 = 3 \cdot 8$, which would make accurate measurement much easier.

3.1.2. *Comparison with flight-test results* (*Fig.* 4).—Only one set of flight-test results is available at present, namely those of Chauvin and de Moraes[18] on a parabolic arc body of revolution of fineness ratio 12·2. (NACA RM-10). The flight plan was such that the skin temperatures increased to maxima and then decreased. The maximum temperatures were taken to be those of zero heat transfer and recovery factors calculated from them are shown by the plain (un-ringed) symbols in Fig. 4. Three values are in the region of the theoretical laminar recovery factor $\sigma^{1/2}$ (assuming $\sigma = 0 \cdot 72$), the remainder are in the region of the turbulent value $\sigma^{1/3}$, but do not follow the decrease with increasing Reynolds number found in the wind-tunnel results of Fig. 2. A further point is that while laminar recovery factors were obtained over the forward portions of both models of the RM-10, the estimated heat-transfer rates for the same regions were those of a fully turbulent flow.

Now the skin thickness of the RM-10 varied appreciably along its length and longitudinal temperature gradients existed as shown in Fig. 21. The effect of such gradients on the local temperatures for zero heat transfer is considered in section 5.2.1.1. and a very rough correction for them would reduce the recovery factors on RM-10, model A, to the values shown by the ringed symbols in Fig. 4. It is obvious from the magnitude of the correction that no definite conclusions can yet be drawn concerning the values of temperature recovery factor in flight and neither can it be said that the recovery factors over the forward portion of the RM-10 are indicative of a laminar boundary layer.

3.13. *Effect of Mach number*.—3.1.3.1. *Laminar boundary layer*.—Crocco's analysis[20], resulting in equation (8) for the recovery factor of a laminar boundary layer, involved placing certain restrictions on the thermal properties of the fluid, including constancy of Prandtl number. Later analyses by Klunker and Mclean[23,55] and by Young and Janssen[24] have removed these restrictions and using experimental values[6] for the variation of specific heat, thermal conductivity, viscosity and Prandtl number, the flow properties have been calculated over a range of Mach number for an ambient temperature of about -55 deg C (*i.e.*, for flight in the stratosphere). The resulting variation of laminar recovery factor is given in Fig. 5 by curve A and shows a marked decrease for Mach numbers greater than two. This decrease is linked with the variation in the properties of air at the high temperatures attained in the boundary layer during flight at high Mach numbers. Also shown for comparison, is curve B, which results from taking $\beta = \sigma^{1/2}$ where σ is evaluated at the surface temperature appropriate to the Mach number in question (using an iteration process and values of σ from Ref. 6) instead of taking σ constant and equal to $0 \cdot 72$. Comparing curve B with curve A indicates that the decrease in recovery factor found by Klunker and McLean[23,55] and by Young and Janssen[24] cannot be obtained by the simple device of altering the temperature level at which σ is evaluated for insertion in the formula $\beta = \sigma^{1/2}$. (At high Mach numbers, curve B tends asymptotically to the value $0 \cdot 806$, whereas curve A continues to decrease, *e.g.*, to $0 \cdot 66$ at $M = 10$)*.

Now curve A is appropriate to flight conditions, and the only flight test results available are those for the RM-10[18] (shown in Fig. 5), which suffer from the defects of temperature gradients as already discussed, but in any case they are not at a sufficiently high Mach number to check the theoretical predictions†.

On the other hand, for the low static temperatures found in conventional supersonic wind tunnels, the air in the boundary layer is not heated much above normal atmospheric temperature so that curve A would not apply. Indeed the mean values of recovery factor obtained from wind-tunnel tests (Figs. 2 and 3) on bodies of revolution, which are plotted in Fig. 5, lie close to the value $\sigma^{1/2}$ with $\sigma = 0 \cdot 72$ up to $M = 3 \cdot 7$. It may be noted that this would correspond roughly to evaluating σ at surface temperature.

It is evident therefore that a considerable amount of work remains to be done on temperature recovery factors, and experimental evidence is particularly required in the flight case for Mach numbers greater than two.

Finally, curve A of Fig. 5 is for the actual zero heat-transfer temperature. The theories[23,24,55] indicate that the datum temperature for use in the heat-transfer coefficient (equation (7)) varies with the temperature of the body surface (T_w), being near to that appropriate to a recovery factor of $0 \cdot 85$ when $T_w = T_1$ and approaching curve A as T_w approaches T_{w0}‡.

3.1.3.2. *Turbulent boundary layer.*—Tucker and Maslen[25] have extended Squire's analysis[22] by allowing for the variation of density across the turbulent boundary layer and their results are shown in Fig. 5. They predict a decrease in temperature recovery factor with increase of Mach number, but the decrease is much less than that predicted[23,24] for the laminar boundary layer. (However, the analysis is much less rigorous than that which can be applied to the laminar boundary layer).

Two points arise concerning the theoretical curves. First, the smaller the value of n, the less the decrease of recovery factor with Mach number becomes. Second, they should be applicable both to flight and to wind-tunnel conditions.

However, comparison with the available experimental results shows no evidence of a decrease of recovery factor with increasing Mach number. It is likely that the possible variation with Reynolds number (Figs. 2 and 3) may be of greater importance.

---

* (1956). These difficulties are overcome if enthalpy is substituted for temperature in the formulae for recovery factor (equation 3) and heat-transfer coefficient (equation 7). A good approximation is then given[62] by evaluating Prandtl number at the temperature corresponding to intermediate enthalpy (equation 12 below, with enthalpy substituted for temperature).

† As already mentioned, these predictions[23,24,55] are based on the properties of air tabulated in Ref. 6. Recently, Bloom[56] has demonstrated how very dependent the results are on the particular values taken for these properties and calls for further experimental determinations of the physical properties of air at high temperatures.

‡ *See* 1956 footnote to section 3.1.3.1., para. 1.

3.1.4. *Suggestions for further work required.*—It seems from the above that the main need is for flight test results:

(*a*) at Reynolds numbers greater than 10 million for all Mach numbers

(*b*) for local Mach numbers greater than two with a laminar boundary layer.

The latter would involve high-altitude flights and careful isolation of the radiation component of heat transfer, since the maximum temperatures reached by the skin will be equilibrium and not zero heat-transfer temperatures.

3.2. *Wires with Axes Perpendicular to the Stream Direction.*—The main interest in this case is in connection with instruments such as the hot-wire anemometer. An immediate difficulty is that the diameter of the wire is usually so small that it will operate in the slip flow region ($\sqrt{(Re/M)} < 100$) unless the Mach number is very low. As a result it is difficult to correlate results obtained with wires of different sizes at different Mach numbers, but Johnson and Rubesin[1] were successful in the case of a $\frac{1}{2}$ mm ($0 \cdot 0197$ in.) wire over a range of Mach numbers from $0 \cdot 4$ to $3 \cdot 3$. Their correlation was based on the wind-tunnel results of Eckert and Weise[26,27] at subsonic speeds and of Eber[28] at supersonic speeds and is reproduced in Fig. 6. (The values of $\sqrt{(Re/M)}$ are not immediately available, but it seems likely that they were on the borderline between the continuum and the slip flow regions).

A partial explanation of the shape of the curve in Fig. 6 for the overall recovery factor of the $0 \cdot 0197$ in. wire can be given from consideration of local recovery factors obtained on cylinders of greater diameter (*e.g.*, Refs. 26, 27). At low subsonic speeds there is very little recovery of temperature on the leeward side of a cylinder; in fact it is possible to record temperatures less than the free-stream static temperature. As a result, the overall temperature recovery factor is low. However, soon after the maximum local Mach number on the cylinder reaches unity (corresponding to free-stream Mach numbers in the region $0 \cdot 5$ to $0 \cdot 6$) the temperature recovery over the rear of the cylinder improves until at supersonic speeds Eber's results[28] give temperatures which are fairly uniform over the whole of the cylinder. Therefore when the Mach number exceeds $0 \cdot 5$ to $0 \cdot 6$, the overall temperature recovery factor will begin to increase and might be expected to level out at supersonic speeds. This is the trend shown by the curve for the $0 \cdot 0197$ in. wire in Fig. 6, but the decrease at low subsonic Mach numbers is not understood.

However, a wire of this size would have too great a thermal lag to be used in hot-wire anemometry. Added in Fig. 6 for comparison are results obtained in a supersonic wind tunnel by Kovásznay[29] for wires of diameters $0 \cdot 0003$ in. and $0 \cdot 00015$ in. These results are definitely in the slip flow region since the values of $\sqrt{(Re/M)}$ are less than ten, and as might be expected they cannot be correlated on the basis of Mach number alone.

3.3. *Temperature Rise at a Stagnation Point.*—If conduction along the length of a body were negligible, then it might be expected that the stagnation point would experience the full stagnation temperature rise given by equation (1). The subsonic experimental results of Eckert and Weise[26,27] support this view for insulated cylinders with their axes perpendicular to the air stream.

However, recent theoretical work by Nonweiler[30] for thin-skinned bodies suggests that heat conduction within the skin can cause the temperature of the nose to be less than the stagnation temperature by an amount which is appreciable at high Mach numbers. Experimental verification is obviously desirable.

4. *Correlation of Heat-Transfer Results.*—In this section we shall consider the degree of correlation of experimental heat-transfer results from wind tunnels and flight which can be obtained on the basis of theories which assume no pressure or temperature gradients along

the length of the body. In many applications the pressure gradients are either zero or are sufficiently small to be neglected, but the same considerations may not be applicable to the temperature gradients and some effects of the latter will be considered in section 5.

In the analysis of experimental results it has been customary to assume recovery factors of the order of $0 \cdot 85$ for laminar and $0 \cdot 90$ for turbulent boundary layers if experimental values for the tests are not available.

4.1. *Laminar Boundary Layers.*—4.1.1. *Theoretical considerations.*—It has been demonstrated by Crocco[20] that the relation:

$$k_H \sigma^{2/3} = \tfrac{1}{2} c_f \quad \ldots \quad (10)$$

between heat-transfer coefficient k_H (equations (5) and (7)) and skin-friction coefficient c_f is approximately true in compressible as well as in incompressible flow. This is verified by the calculations of Klunker and McLean[23,55] for flight at high Mach numbers and in addition their values for skin-friction coefficient are close to those obtained by an extension of Crocco's analysis[20] (for constant Prandtl number) at least up to $M = 10$. On the other hand, modifications may need to be made to the effective temperature difference used in forming the coefficient k_H (section 3.1.3.1)*. However, the local Mach numbers obtained in flight tests to date do not extend into this region.

Young[31] and also Johnson and Rubesin[1] have obtained semi-empirical formulae which approximate to Crocco's skin-friction results[20] for a flat plate in compressible flow. These formulae are compared in Ref. 32 and either could be used for correlating experimental results. However, the only available results are those of Fischer and Norris[34] and their analysis was based on the Johnson and Rubesin formula, so for convenience the same formula will be used in the present note. It is (for local skin friction):

$$c_f' = 0 \cdot 664 (Re_x')^{-1/2}, \quad \ldots \quad (11)$$

where the primes denote that density and viscosity are to be evaluated at an 'intermediate' temperature:

$$T' = 0 \cdot 42 T_1 (1 + 0 \cdot 076 M_1^2) + 0 \cdot 58 T_w . \quad \ldots \quad (12)$$

These equations should be applicable as they stand to a cylinder with axis in the stream direction[33], but for supersonic flow over a cone the constant in equation (11) should be increased[33] by the factor $\sqrt{3}$ to $1 \cdot 15$.

4.1.2. *Experimental results.*—The only available experimental results for heat transfer in high-speed flow with a laminar boundary layer are those of Fischer and Norris[34]. Local heat-transfer coefficients were calculated from the measured variations during flight of the skin temperatures on the nose cones of V-2 type missiles. A correlation on the basis of equations (10) and (11) (with constant increased to $1 \cdot 15$) and (12) is reproduced in Fig. 7. (In equation (10), Fischer and Norris evaluated σ at temperature T' and this is repeated in Fig. 7).

In the case of V-2 No. 27, the nose cone had an included angle of 45 degrees, and the local Mach number increased from 1 to 3 as the altitude increased from 30,000 to 100,000 ft. Because of the flight plan the Reynolds numbers decreased as time increased, so that the laminar results were obtained during the later portion of the measured flight and a time scale in Fig. 7 would run from right to left. Zero heat-transfer conditions were not achieved, so a recovery factor of the order of $0 \cdot 85$ was assumed in the analysis.

* *See* 1956 footnote to section 3.1.3.1., para 1.

Considering the correlation in Fig. 7, apart from a decrease at the end of the measured flight, the average values of the experimental heat-transfer coefficients for V-2 No. 27 are about 20 per cent above the theoretical curve.

On the other hand the results from the firing of V-2 No. 21 lie much closer to the theoretical curve. (Complete details of this firing are not available).

In general therefore it can be said that, apart from the unexplained tailing-off of the results from V-2 No. 27, the theoretical formula gives a reasonable approximation to the experimental results and further evidence would be needed before improvements could be justified.

4.1.3. *Simplified formula for general use.*—Suppose that in equations (10) and (11) we evaluate density and viscosity at the surface temperature T_w instead of at the intermediate temperature T' of equation (12). We then obtain:

$$k_{Hw}\sigma_w^{2/3} = 0\cdot 332 Re_w^{-1/2} \qquad \ldots \quad \ldots \quad \ldots \quad \ldots \quad \ldots \qquad (13)$$

or, in terms of local conditions outside the boundary layer:

$$k_H\sigma_w^{2/3} = 0\cdot 332 Re^{-1/2}(T_1/T_w)^{\{(1-\omega)/2\}} \qquad \ldots \quad \ldots \quad \ldots \qquad (14)$$

if it is assumed that:

$$\frac{\mu_1}{\mu_w} = \left(\frac{T_1}{T_w}\right)^\omega . \qquad \ldots \quad \ldots \quad \ldots \quad \ldots \quad \ldots \quad \ldots \qquad (15)$$

Fig. 8 compares heat-transfer coefficients obtained from equation (13) (or (14)) with those obtained from the 'true' formula of equations (10), (11) and (12) and shows that up to $M_1 = 6$ and over a feasible range of surface temperatures the errors introduced should not exceed 5 per cent. Equation (13) (or (14)) should therefore be sufficiently accurate for general use and is more simple in application than the 'true' formula based on intermediate temperature.

Similar considerations would apply to mean heat-transfer coefficient.

4.2. *Turbulent Boundary Layers.*—4.2.1. *Theoretical and incompressible flow considerations.*—4.2.1.1. *Skin friction.*—The various formulae which have been proposed for the variation of turbulent skin friction in compressible flow with zero longitudinal pressure and temperature gradients have already been reviewed in Ref. 5, where it is shown that the relations[35]:

$$\left.\begin{aligned} c_{fi} &= c_{fw} \\ \text{when} \qquad Re_i &= Re_w \frac{T_1}{T_w} \end{aligned}\right\} \qquad \ldots \quad \ldots \quad \ldots \quad \ldots \quad \ldots \quad \ldots \qquad (16)$$

(where subscript $_i$ denotes incompressible-flow values) give a sufficiently accurate approximation to more complicated formulae*. These relations can be applied to any of the formulae for turbulent skin friction in incompressible flow to provide a corresponding formula for compressible flow. In the region $10^6 < Re < 10^8$ a suitable formula (for flat plates) for local skin friction

* (1956). It has now become apparent that equations 16 may seriously overestimate skin friction and heat transfer at high Mach numbers if the surface temperature is low. It is preferable to use the 'intermediate enthalpy' approach throughout (*see* Refs. 62 and 63), but if equations 16 are used, they should be subjected to the restriction that $T_w/T_{H1} \geqslant \frac{1}{2}$.

The remainder of section 4.2 should be viewed in this light.

is the Blasius formula[21] $c_{fi} = 0 \cdot 0592 Re_i^{-1/5}$ which, when transformed according to equations (16) becomes:

$$c_{fw} = 0 \cdot 0592 \left(Re_w \frac{T_1}{T_w} \right)^{-1/5} \quad \ldots \quad (17)$$

or in terms of local stream values:

$$c_f = 0 \cdot 0592 Re^{-1/5} \left(\frac{T_1}{T_w} \right)^{(3-\omega)/5} \quad \ldots \quad (18)$$

where ω is defined by equation (15).

Similarly, the mean skin-friction coefficient is given by:

$$C_{Fw} = 0 \cdot 074 \left(Re_w \frac{T_1}{T_w} \right)^{-1/5} \quad \ldots \quad (19)$$

and presumably the range of validity of equations (17) and (19) should now be taken as $10^6 < Re_w(T_1/T_w) < 10^8$.

The Blasius formula possesses the merits of simplicity but if greater accuracy over a wider range of Reynolds numbers is required, then incompressible-flow results[21] would suggest the use of Prandtl-Schlichting–type formulae which when modified in accordance with equation (16) give:

$$c_{fw} = 0 \cdot 288 \left(\log_{10} Re_w \frac{T_1}{T_w} \right)^{-2 \cdot 45} \quad \ldots \quad (20)$$

for local skin friction and:

$$C_{Fw} = 0 \cdot 46 \left(\log_{10} Re_w \frac{T_1}{T_w} \right)^{-2 \cdot 6} \quad \ldots \quad (21)$$

for mean skin friction in compressible flow. The probable range of application is $10^5 < Re_w(T_1/T_w) < 10^9$, corresponding to the whole range of available incompressible-flow experimental results.

In the above, Reynolds numbers are based on length along the surface of the body. If, as in Ref. 37, they are based on boundary-layer thickness, then the same analysis[35] which led to equation (16) gives, in this case:

$$\left. \begin{array}{l} c_{fi} = c_{fw} \\ \text{when} \quad R_{\delta i} = R_{\delta w} \end{array} \right\} \quad \ldots \quad (22)$$

i.e., the additional factor T_1/T_w is no longer attached to the compressible-flow Reynolds number.

4.2.1.2. *Relations between heat-transfer and skin-friction coefficients.*—Turning now to the relation between heat-transfer and skin-friction coefficients, Fig. 9 shows various values which have been proposed or used under incompressible-flow conditions, assuming $\sigma = 0 \cdot 72$. Of these, the Karman relation[21] has the most logical foundation, being based on the measured structure of the turbulent boundary layer and it may be noted that a reasonable approximation to it in the range $10^6 < Re_i < 10^8$ is given by:

$$\frac{k_H}{\frac{1}{2}c_f} = \sigma^{-1/3} . \qquad \ldots \quad \ldots \quad \ldots \quad \ldots \quad \ldots \quad \ldots \qquad (23)$$

If we assume that equation (23) can also be applied in compressible flow*, there is the question as to the temperature at which σ should be evaluated. However, since according to Ref. 6, σ only varies from $0 \cdot 73$ at -50 deg C to a minimum of $0 \cdot 65$ at temperatures greater than 500 deg C, this may not be very important compared with possible errors from other sources. In the correlations which follow, it has arbitrarily been evaluated at the surface temperature T_w.

4.2.2. *Experimental results.*—4.2.2.1. *Overall heat transfer.*—Fig. 10 gives the results of measurements of the overall heat transfer from a flat plate mounted in a supersonic wind tunnel[9,10], plotted as mean heat-transfer coefficient $\bar{k}_{Hw}$ against the modified Reynolds number $Re_w(T_1/T_w)$ as suggested by equation (16).

As Fig. 10 shows, the values of $Re_w(T_1/T_w)$ are outside the range for which the power-law formula of equation (19) would be recommended by skin-friction results in incompressible flow[21]. Despite this fact, a slightly better correlation could be obtained using this formula than by use of the log-formula of equation (21), and Fig. 10 then shows the effects of applying the various relations of Fig. 9 between heat transfer and skin friction. The experimental results lie between the curves derived from the Karman relation and the $\sigma^{-2/3}$ relation as used by Colburn. (Corresponding curves derived from the log-formula of equation (21) would be about 6 per cent lower in each case at $Re_w(T_1/T_w) = 10^5$. The experimental results would then favour the $\sigma^{-2/3}$ relation).

Prandtl number was taken as $0 \cdot 72$, which corresponds to the surface rather than the stream temperatures. The latter were outside the range for which tabulated values of Prandtl number exist[6].

4.2.2.2. *Local heat transfer.*—Local heat-transfer coefficients obtained both from wind-tunnel and from flight measurements are plotted in Figs. 11 and 12 against $Re_w(T_1/T_w)$ as suggested by equation (16). The sources of the experimental data are listed in the figures, as are the ranges of local Mach number covered.

The thermal properties of air have been evaluated at surface temperatures T_w and the heat-transfer coefficients k_{Hw} have been multiplied by the factors described in section 4.2.1.2. to reduce them to 'equivalent skin-friction coefficients' for comparison with the power-law formula of equation (17). Fig. 11 is based on the $\sigma^{1/3}$ factor, which approximates to the Karman relation (*see* Fig. 9), and Fig. 12 is based on the $\sigma^{2/3}$ factor as used by Colburn.

Also, two curves have been drawn in Fig. 11, one for flat plates (equation (17)) and the other for cones in which the flat-plate constant is increased by the factor $(3\sqrt{3})/4$ as found by Davies[17]. In Fig. 12, only the flat plate curve has been drawn.

Comparison of Figs. 11 and 12 shows that a slightly better correlation is achieved using the $\sigma^{2/3}$ factor of Fig. 12, *i.e.*,

$$\frac{k_{Hw}}{\frac{1}{2}c_{fw}} = \sigma_w^{-2/3} \qquad \ldots \quad \ldots \quad \ldots \quad \ldots \quad \ldots \quad \ldots \qquad (24)$$

* A recent analysis[57] by Rubesin for the case of compressible flow gave values of $k_H/\frac{1}{2}c_f$ about 7 per cent on average above those given by the Karman relation in Fig. 9. Rubesin included an 'effective Prandtl number' for the turbulent flow, which he evaluated by means of the temperature recovery factor, but in doing this he had to simplify the structure of the boundary layer by omitting the buffer layer between the laminar sub-layer and the turbulent core. This omission corresponds to the Taylor-Prandtl assumption for incompressible flow, which in that case gives values of $k_H/\frac{1}{2}c_f$ about 3 per cent below those from the Karman relation.

and when this is done, the flat-plate formula of equation (17) gives reasonable agreement with the experimental results. Apart from experimental inaccuracies, much of the scatter and indeed the general level of the experimental results may be affected by temperature gradients along the length of the test bodies (*see* section 5 below), but ignoring these, the heat-transfer formula:

$$k_{Hw}\sigma_w^{2/3} = 0\cdot0296\left(Re_w\frac{T_1}{T_w}\right)^{-1/5} \quad \ldots \quad \ldots \quad \ldots \quad \ldots \quad (25)$$

(derived from equations (17) and (24)) may be regarded as sufficiently accurate for use in calculating skin temperature variations, at least until further experimental evidence (preferably from flight tests) makes improvement possible*.

Significance of equation (25).—In terms of local free-stream (local ambient) conditions, equation (25) becomes:

$$k_H\sigma_w^{2/3} = 0\cdot0296Re^{-1/5}\left(\frac{T_1}{T_w}\right)^{(3-\omega)/5} \quad \ldots \quad \ldots \quad \ldots \quad \ldots \quad (26)$$

where ω is given by:

$$\frac{\mu_1}{\mu_w} = \left(\frac{T_1}{T_w}\right)^{\omega} \quad \ldots \quad \ldots \quad \ldots \quad \ldots \quad \ldots \quad \ldots \quad (15)$$

(σ_w is still to be evaluated at surface temperature T_w).

The point of note in equation (26) is that the compressibility parameter is T_w/T_1 and therefore it is only under zero heat-transfer conditions ($T_w = T_{w0}$, *see* section 3) that Mach number is of importance. This is illustrated by Fig. 13, where flight test results from RM-10 firings[18,37] are plotted first against Mach number and then against the ratio T_w/T_1. The ordinate in each case is the ratio of the heat-transfer coefficient (multiplied by $\sigma_w^{2/3}$) obtained in the tests to the incompressible-flow value at the same Reynolds number as estimated by equation (26) with $T_w = T_1$. This is a sensitive method of plotting, which explains the apparent increase in scatter when compared with Fig. 12, but T_w/T_1 is obviously the better choice of compressibility parameter. A consequence of this is that if the surface is cold ($T_w \simeq T_1$) then the heat-transfer coefficient may not be reduced much below its incompressible-flow value even though the body may be flying at a high Mach number†.

Practical significance of errors in heat-transfer coefficient.—Finally one effect of errors in heat-transfer coefficient is illustrated by Fig. 14, where measured skin temperatures on the RM-10 are compared with values estimated by the step-by-step calculation procedure of Ref. 45, using local heat-transfer coefficients given by the flat-plate curve of Fig. 11 which are on average 20 per cent below the experimental coefficients. The two stations correspond to those used in the correlations of Figs. 11 and 12.

Measured temperatures for these stations are only available onwards from a time of 4 seconds, but for some other stations the initial temperature was about 27 deg C so in the first place it was assumed that the whole of the surface was initially at the same temperature, *i.e.*, 27 deg C. Half-second time intervals were used in the calculations. This led to the curves marked A in Fig. 14.

* *Note* 1956 footnote to section 4.2.1.1. Also *see* Ref. 64, which supports a value $k_H/\frac{1}{2}c_f \simeq 1\cdot22$.

† *Note* 1956 footnote to section 4.2.1.1.

First considering station 123·5 (inches from tip), Fig. 14 shows that the calculated and measured temperatures are within 5 deg C, despite the 20 per cent difference between heat-transfer coefficients. This measure of agreement should be adequate for most engineering purposes.

However, there is up to 30 deg C difference between the results at station 17·8, despite the fact that the difference between experimental and assumed heat-transfer coefficients is still of the order of 20 per cent (*see* Fig. 11, unflagged symbols). It is unlikely that the initial temperature at this station was much higher than 27 deg C, and a repeat of the calculations using one-fifth–second time intervals did not reduce the discrepancy. The calculations for station 17·8 were then repeated for the measured portion of the flight, assuming an initial temperature of 180 deg C at a time of 4 seconds. The result (given by curve B in Fig. 14) shows the same order of agreement with experiment as was found with curve A at station 123·5, so it is obvious that there must have been a very much high rate of heat flow into station 17·8 during the first 4 seconds of the flight than would be accounted for by a 20 per cent increase in heat-transfer coefficient.

Further experimental evidence from flight tests is highly desirable and it is suggested that the true worth of any formula for heat-transfer coefficient is best assessed by comparing calculated and measured skin-temperature histories as in Fig. 14.

5. *Effects of Temperature Gradients on Local Heat-Transfer Coefficients*.—5.1. *Effect of a Stepwise Discontinuity in Surface Temperature*.—This is a case frequently met in wind-tunnel tests, when it may not be possible to heat (or cool) the test body right forward to its tip or leading edge. As a result the temperature of the forward portion of the body may remain close to the zero heat-transfer condition and it will then take some length of run for the boundary layer to acclimatise itself to the subsequent heated portion. The local heat-transfer coefficients over the heated portion can therefore differ from those which would be measured on a surface having uniform temperature all the way from the tip or leading edge.

In the present section we shall assume uniform temperature over the heated portion, so that we have the case of a single stepwise discontinuity in surface temperature.

5.1.1. *Laminar boundary layer*.—If we assume that conditions are as illustrated by the sketch inset in Fig. 15 and that the local skin-friction coefficient retains values appropriate to uniform temperature, then applying the formula (equation (29) below) obtained by Lighthill for the laminar boundary layer in compressible flow[42], we obtain:

$$\frac{k_H}{k_{H0}} = \left[1 - \left(\frac{x_1}{x}\right)^{3/4}\right]^{-1/3} \qquad \ldots \quad \ldots \quad \ldots \quad \ldots \quad \ldots \quad (27)$$

for the local heat-transfer coefficient k_H at a distance x from the leading edge, where x_1 is the length of the unheated portion and k_{H0} is the value of k_H for uniform temperature conditions ($x_1 = 0$), as given by equation (14) for example.

The curve given by equation (27) for k_H/k_{H0} is plotted in Fig. 15 against $(1 - x_1/x)$, i.e., ratio of heated to total length, and shows the considerable effect that the discontinuity can have.

Fig. 16 then shows an application of equation (27) (or Fig. 15) to experimental results obtained by Brun[38] from an ogive-cylinder in a supersonic wind tunnel. Only the cylindrical portion was heated (to temperatures around 800 deg C) and its temperature distribution was reasonably uniform relative to the temperature jump at the junction of the ogive and the cylinder. Further details are given below Fig. 16. The plotted results show that equation (27) (curve of Fig. 15) gives a correction of the right order for the effect of a stepwise temperature discontinuity on the local heat-transfer coefficients for a laminar boundary layer in compressible flow.

5.1.2. *Turbulent boundary layer.*—Lighthill's theory[42] applies to incompressible and compressible laminar boundary layers. A similar theory has not been developed for the compressible turbulent boundary layer, but in the incompressible case Rubesin[40] has obtained the formula:

$$\frac{k_H}{k_{H0}} = \left[1 - \left(\frac{x_1}{x}\right)^{39/40}\right]^{-7/39}, \qquad \ldots \quad \ldots \quad \ldots \quad \ldots \quad (28)$$

where the various symbols are defined as in equation (27). The ratio k_H/k_{H0} as given by equation (28) is plotted against $(1 - x_1/x)$ in Fig. 17, and comparison with Fig. 15 shows that theoretically a stepwise discontinuity in temperature has considerably less effect on a turbulent than on a laminar boundary layer. Also plotted in Fig. 17 are experimental results obtained by Tessin and Jakob[39] from tests on cylinders at low speeds and comparatively low rates of heat transfer. These experimental results are in very good agreement with Rubesin's curve for $(1 - x_1/x) > 0 \cdot 4$.

Once again, compressible-flow results are available from Brun's tests[38]. These are at subsonic speeds but for high temperature differences across the boundary layer, using the same equipment as for the laminar boundary layer results of Fig. 16. The direct results and the effect of correction by equation (28) are shown in Fig. 18, which demonstrates that Rubesin's formula is adequate in this case for dealing with the effect of a stepwise temperature discontinuity on the local heat-transfer coefficients for a turbulent boundary layer in compressible flow.

5.2. *General Temperature Distribution.*—In flight, a thin-skinned body will not in general be at uniform temperature during the transient heating stage because of the variation of heat-transfer coefficient along its length. Conduction of heat along the skin will help to reduce the non-uniformity, but in many cases this reduction may only be appreciable very near to the nose (*see* Ref. 30) or possibly in the transition region between laminar and turbulent flow.

As in the case of the stepwise discontinuity of section 5.1, a non-uniform temperature distribution along the body will modify the boundary layer and affect the heat-transfer coefficents. The most general solution of the problem in the case of a laminar boundary layer is that of Lighthill[42] who obtains (in effect):

$$\frac{k_H}{k_{H0}} = \frac{1}{T_w(x) - T_{w0}} \int_{z=0}^{x} \frac{d\{T_w(z) - T_{w0}\}}{[1 - (z/x)^{3/4}]^{1/3}} \qquad \ldots \quad \ldots \quad \ldots \quad (29)$$

for the local heat-transfer coefficient k_H at a distance x from the leading edge of a flat plate. Other symbols are defined as in equation (27). It is assumed that the leading edge ($x = 0$) is at zero heat-transfer temperature and that the local skin-friction coefficient retains values appropriate to a plate at uniform temperature.

Equation (29) can be applied, for example, to a particular measured temperature distribution to obtain the corresponding modification required in local heat-transfer coefficient as derived from the test results.

A corresponding formula is not available for the turbulent boundary layer, but by comparing equations (29) and (27) for the laminar boundary layer, a possible generalisation of equation (28) for the turbulent boundary layer is indicated to be:

$$\frac{k_H}{k_{H0}} = \frac{1}{T_w(x) - T_{w0}} \int_{z=0}^{x} \frac{d\{T_w(z) - T_{w0}\}}{[1 - (z/x)^{39/40}]^{7/39}} . \qquad \ldots \quad \ldots \quad \ldots \quad (30)$$

The effect of non-uniform surface temperature on the transient aerodynamic heating of thin-skinned bodies, assuming laminar boundary layers, has been studied by Bryson and Edwards[44], who used Lighthill's formula (equation (29)) in their calculations. Fig. 19 reproduces the results they obtained in the case of an exponential decrease of velocity with time at constant altitude with the initial surface temperature constant and less than the initial zero heat-transfer temperature. Fig. 19A shows the local heat-transfer rates at two stations along the body and these are seen to differ greatly from the corresponding values for uniform plate temperature. On the other hand, Fig. 19B shows that the skin temperature variations do not differ to the same extent. The moral would seem to be that considerable scatter can quite easily be 'built-in' to heat-transfer coefficients derived from measured variations of skin temperature during a flight (or intermittent tunnel) test, if the surface temperatures are not uniform along the length of the body. This reinforces the suggestion made at the end of section 4 that the true worth of any formula for heat-transfer coefficient is best assessed by the skin-temperature variations it predicts.

5.2.1. *Approximate results.*—If the temperature distribution along the body can be represented by a polynomial then Chapman and Rubesin[43] and Rubesin[40] have developed series solutions for heat transfer with laminar and turbulent boundary layers respectively. These are necessarily more restricted in application than the integral formulae of equations (29) and (30), but they can conveniently be used to illustrate the major effects of a non-uniform temperature distribution.

In both cases[40,43] the surface temperature distribution is assumed to be given by*:

$$\frac{T_w}{T_{w0}} = 1 + a_0 + a_1\left(\frac{x}{l}\right) + a_2\left(\frac{x}{l}\right)^2 + \ldots \qquad (31)$$

where l is the overall length of surface and T_{w0} is the zero heat-transfer temperature when the surface temperature is uniform. If so, then the local heat-transfer rate is given by:

$$\frac{q}{h_0 T_{w0}} = a_0 Y_0 + a_1 Y_1\left(\frac{x}{l}\right) + a_2 Y_2\left(\frac{x}{l}\right)^2 + \ldots \qquad (32)$$

where h_0 is the value of h (equation (7)) for uniform temperature and values of the quantities Y_0, Y_1, Y_2, etc., are given in the following table as calculated in Refs. 40 and 43.

Values of Y_n

Quantity	Y_0	Y_1	Y_2	Y_3	Y_4	Y_5	Y_{10}
Laminar boundary layer	1	1·653	2·020	2·313	2·517	2·701	3·402
Turbulent boundary layer	1	1·222	1·343	1·427	—	—	—

There is no reason to restrict n to integral values and, if it is not an integer, Y_n may be obtained by interpolation using the curves of Fig. 20.

5.2.1.1. *Effect on zero heat-transfer condition.*—Suppose that in the region of the zero heat-transfer condition the surface temperature distribution is given by:

$$\frac{T_w}{T_{w0}} = 1 + a_0(t) - a_n\left(\frac{x}{l}\right)^n, \qquad (33)$$

* Ref. 40 considers only the incompressible turbulent boundary layer, but we shall assume that the results can be applied to the compressible-flow case if T_1 is replaced by T_{w0}.

where $a_0(t)$ varies with time. Then from equation (32) we obtain (since $Y_0 = 1$):

$$\frac{q}{h_0 T_{w0}} = a_0(t) - a_n Y_n \left(\frac{x}{l}\right)^n \quad \ldots \quad (34)$$

and at a given point (x/l) the local heat transfer is zero when $a_0(t) = a_n Y_n (x/l)^n$ or, from substitution in equation (33), when:

$$\frac{T_w}{T_{w0}} = \frac{T_{w0}'}{T_{w0}} = 1 + a_n \left(\frac{x}{l}\right)^n \{Y_n - 1\} . \quad \ldots \quad (35)$$

Thus, unless $n = 0$ (uniform temperature), zero heat transfer at the point (x/l) occurs at a temperature T_{w0}' which is different from the value T_{w0} for a surface of uniform temperature. This explains why the heat-transfer coefficients in Fig. 19A, which are based on the temperature difference $(T_w - T_{w0})$, become infinite when $T_w = T_{w0}$.

A further consequence of equation (35) is that if recovery factors are deduced from the maximum values of measured variations of skin temperature with time (such as in Fig. 14), then the results will depend on the distribution of surface temperature.

For example Fig. 21 shows the variation of surface temperature over the RM-10, model A[18], when conditions were near that of zero heat transfer (as deduced from the maximum recorded skin temperatures in plots such as in Fig. 14). In compiling Fig. 21, a recovery factor of 0·9 was assumed when obtaining the values of T_{w0} used in forming the ratio T_w/T_{w0}.

The relatively high values of T_w/T_{w0} over the forward portion of the body are explained by the fact that the skin was thinner in the region $0 < x/l < 0 \cdot 2$ than it was for $x/l > 0 \cdot 2$. Considering the latter region, the temperature distributions were approximated by a linear variation as shown in Fig. 21 and values of T_{w0}'/T_{w0} were obtained from equation (35) with $n = 1$ and $Y_n = 1 \cdot 222$ (turbulent boundary layer). The results are given in Fig. 22 as are the corrections which would be necessary to recovery factors (β') derived from T_{w0}'.

Applying these corrections to the measured recovery factors for the RM-10 in Fig. 4 gives the ringed symbols of that figure, which provide an ample illustration of the errors which may be involved in comparisons between recovery factors obtained on bodies having different distributions of surface temperature.

From the table of values of Y_n it can be seen that the effects of non-uniform surface temperatures will be more pronounced if the boundary layer is laminar than if it is turbulent.

Finally it must be emphasised that the analysis above for the RM-10 is very rough and is only intended as an illustration.

5.2.1.2. *Effect on heat-transfer coefficient.*—It has already been mentioned that local heat-transfer coefficients based on $(T_w - T_{w0})$ will become infinite when $T_w = T_{w0}$, if the surface temperature is not uniform. Therefore it would seem better to base the coefficients on $(T_w - T_{w0}')$. In effect this is done in the analysis of flight tests such as on the RM-10, since the measurements yield the value T_{w0}' for zero heat transfer.

Complications arise since the temperature distribution is likely to be changing continually throughout the flight, but it is of interest to consider conditions near to zero heat transfer, when the distribution may remain sufficiently close to a type such as given by equation (33). If so, then from equations (33) and (35) we obtain $(T_w - T_{w0}')/T_{w0} = a_0(t) - a_n Y_n (x/l)^n$, and if we define $h' = q/(T_w - T_{w0}')$ then from equation (34) we obtain $h'/h_0 = 1$, *i.e.*, the local heat-transfer coefficient h' is the same as would be obtained on a surface of uniform temperature.

However for greater rates of heat transfer (*i.e.*, greater values of $T_w - T_{w0}'$) it will make little difference whether the heat-transfer coefficient is based on $(T_w - T_{w0}')$ or on $(T_w - T_{w0})$ and variations such as for the higher values of t/t_0 in Fig. 19 may be expected if the temperature distribution is changing. Once again the effects would be less if the boundary layer were turbulent.

5.3. *Conclusions.*—(*a*) If there is a variation in surface temperature along a body, then the zero heat-transfer temperature (T_{w0}') at any point will differ from that obtained on a surface of uniform temperature.

(*b*) If the distribution of surface temperature remains fixed then local heat-transfer coefficients based on $(T_w - T_{w0}')$ should not differ much from those obtained on a surface of uniform temperature.

(*c*) In the general case the integral formula of equation (29)[42] may be used to determine variations in k_H for a laminar boundary layer and it is suggested that equation (30) may be applicable to the turbulent boundary layer.

6. *Effect of Pressure Gradients on Heat-Transfer Coefficients.*—No systematic work has yet been done on this case. Theories exist for the laminar boundary layer in compressible flow with pressure gradients under zero heat-transfer conditions (*e.g.*, Ref. 46), but so far there has been no rigorous extension of the theory to include heat-transfer conditions. Even less is known about the behaviour of the turbulent boundary layer and some recent low-speed work (unpublished) at the Oxford University Engineering Laboratory suggests that the relation between heat-transfer and skin-friction coefficients may alter appreciably when pressure gradients are present.

Now except near the tail of a body or the trailing edge of a wing, the pressure gradients are likely to be small on aircraft or missiles designed for supersonic flight. There was a small favourable pressure gradient over the length of the RM-10[18] (a body of fineness ratio 12·2) but an attempt made by Rubesin, Rumsey and Varga[3] to allow for its effects yielded local heat-transfer coefficients very little different from those obtained from a uniform-flow type of analysis (*e.g.*, Fig. 12). Further evidence is provided by Fraenkel[58], who made approximate calculations of the boundary-layer development under zero transfer conditions on a body of revolution (a cone-cylinder with various truncated parabolic afterbodies) and obtained overall skin-friction coefficients close to those given by a flat-plate formula over a range of Mach numbers from 1·2 to 1·6 and of Reynolds numbers from 48 to 72 million. In this case the fineness ratios were between 14·5 and 17.

Therefore, until further evidence becomes available it would seem reasonable to assume that at least for the turbulent boundary layer, uniform-flow formulae may suffice for bodies with fineness ratios of the order of 12 or more. However, systematic experimental results are obviously highly desirable.

7. *Transition from Laminar to Turbulent Flow.*—The previous sections have considered the heat transfer rates obtained with wholly laminar or with wholly turbulent boundary layers. In supersonic flight at low altitudes it may be sufficiently accurate in many cases to assume a wholly turbulent boundary layer, neglecting the influence of the probably short run of laminar boundary layer near the nose. Thus, for example, at sea level and for a speed of 2,000 ft/sec the Reynolds number per foot is of the order of 13 million so that extensive laminar boundary layers are unlikely (but *see* section 7.1 below for possible modification of this statement).

However, as the altitude increases the Reynolds number decreases, until at 100,000 ft (and 2,000 ft/sec) it is only of the order of 0·2 million per foot, so that it becomes increasingly important to know how transition may vary during the flight.

Gazley[4] has already made a fairly detailed review of the problem, so that only a general statement will be made in the present section. The main purpose is to emphasise some of the major factors which affect transition and to present what is in some cases a slightly different interpretation of the experimental results from that given by Gazley[4].

The factors which will be considered are:

(*a*) the effect of heat transfer

(*b*) the effect of pressure gradients

(*c*) the effect of incidence

(*d*) the effect of single spanwise roughness elements.

Some consideration is also given to the effect of turbulence level in a wind tunnel.

Shock waves (such as from a wing on to a body) may have considerable effect in fixing transition, but as yet there is very little experimental evidence available. (A few results, incidental to their main investigation have been obtained by Gadd, Holder and Regan during their work on shock-wave–boundary-layer interaction[54]).

7.1. *Effect of Heat Transfer*.—7.1.1. *Theoretical considerations*.—Gazley[4] gives a good review of the theory of boundary-layer stability in low-speed flow. Briefly there have been two main starting points. One, suggested by G. I. Taylor, supposes that turbulence in the stream outside the boundary layer imposes local adverse pressure gradients on the laminar boundary layer which cause local separation and subsequent transition to turbulent boundary-layer flow. The other, developed by Tollmien and Schlichting, considers the stability of small disturbances in the boundary layer. These disturbances may be caused by surface roughness, noise, vibration, or free-stream turbulence, and they make their appearance as oscillations which may be damped out or amplified depending on their frequency and the local Reynolds number. For a given frequency, amplification can only occur if the Reynolds number is greater than a certain value known as the 'minimum critical Reynolds number', and if this is so, then after a certain distance the oscillations become amplified to such an extent that they break up into irregular fluctuations and the boundary layer becomes turbulent.

Low-speed experimental results (such as those of Schubauer and Skramstad) have shown that the level of the free-stream turbulence decides which mechanism is the prime cause of transition. This is illustrated by Fig. 29 (taken from Ref. 4) which is a plot of the mean values of experimentally determined transition Reynolds numbers in low-speed flow against the turbulence level of the free stream (u'/u_1). Fig. 29 shows that for u'/u_1 greater than about $0 \cdot 001$, transition is affected by the turbulence level of the wind tunnel (as suggested by G. I. Taylor), but for smaller values the turbulence level has negligible effect and in fact it was found that transition was caused by the amplification of Tollmien-Schlichting waves.

Now the theories[47, 48, 52] which have been developed for the stability of the laminar boundary layer in compressible flow have all been based on the Tollmien-Schlichting assumption. On the other hand, turbulence levels have not yet been measured in any of the supersonic wind tunnels from which transition measurements are available, so that when comparing the experimental trends with the theoretical predictions, the implications of Fig. 29 must be borne in mind.

In extending the Tollmien-Schlichting theory to compressible flow, Lees[47] found the interesting result that heat transfer has a major effect on the values of the minimum critical Reynolds number Re_c. Heating (heat transfer from body to air stream) reduces Re_c, but cooling (heat transfer from air stream to body) increases it and in supersonic flow if the cooling rate is sufficient then Re_c becomes infinite, *i.e.*, the laminar boundary layer becomes completely stable. In obtaining these results, approximations had to be made in the solution of the boundary-layer stability equations and in view of the importance of Lees' results, further studies have been made with the aim of improving their accuracy. The latest of these is by Van Driest[48], whose main results are summarised in Figs. 23 to 25*.

Fig. 23 shows the theoretical cooling requirements for complete stability of the laminar boundary layer, plotted as the ratio of the required surface temperature to the zero heat-transfer temperature against Mach number. All temperature ratios below the curve correspond to complete stability and it is seen that this is most easily obtained in the neighbourhood of $M = 2$, whereas at higher Mach numbers it becomes increasingly more difficult until above $M = 9$ it is impossible to obtain.

Fig. 24 is a plot of the minimum critical Reynolds number under zero heat-transfer conditions, which shows that Mach number has a destabilising effect.

Using Fig. 24 and Van Driest's results for the effects of heat transfer, Fig. 25 was obtained, which gives curves of the ratio (minimum critical Reynolds number/minimum critical Reynolds number under zero heat-transfer conditions) against the surface temperature ratio T_w/T_{w0} for constant values of Mach number. In application to the flight case, the cooling region is of major importance and it is worth noting that cooling is most effective in the range $1 \cdot 5 < M < 2 \cdot 5$. (The asymptotes to the curves in Fig. 25 are at the values of T_w/T_{w0} given in Fig. 23).

Now Figs. 23 to 25 give minimum critical Reynolds numbers Re_c and as yet these cannot be related to the transtition Reynolds numbers Re_T. However, the same qualitative trends might be expected if the free-stream turbulence level is low enough for the theory to be applicable. Summarising, these trends are:

(*a*) under zero heat-transfer conditions ($T_w/T_{w0} = 1$) Re_T may decrease as the Mach number increases (Fig. 24).

(*b*) cooling ($T_w/T_{w0} < 1$) may delay transition (increase Re_T) and may be most effective in the range $1 \cdot 5 < M < 2 \cdot 5$ (Fig. 25)

(*c*) heating ($T_w/T_{w0} > 1$) may decrease Re_T and its effects may be more appreciable at the lower supersonic Mach numbers (Fig. 25).

7.1.2. *Experimental results.*—Experimental results both from flight and wind-tunnel tests are given in Fig. 26 in the form of a semi-logarithmic plot of transition Reynolds number (Re_T) against the temperature ratio T_w/T_{w0}. The Reynolds numbers and quoted Mach numbers are based on local stream conditions.

Considering the flight-test results, the very high transition Reynolds numbers obtained by Sternberg[49] were on a specially polished nose-cone fitted to a V-2–type missile with trajectory modified to give a flight at approximately constant altitude (25,000 ft). Angles of pitch and yaw were measured and were less than ± 1 degree after the missile had levelled out at altitude. Unfortunately the missile exploded (from unknown causes) before zero heat-transfer conditions were reached. Transition was deduced from a change in slope in plots of measured skin temperatures against time and Sternberg himself only quotes the highest value shown in Fig. 26. The remainder were deduced by the present author and there can be some doubt concerning the accuracy both of the values shown and of the extrapolation to zero heat-transfer conditions.

* (1956). Further calculations have since been made, allowing for variations in Prandtl number, etc. These make some alterations in values but do not affect the overall shapes of Figs. 23 to 25. More important modifications arise from the work of Dunn and Lin[65], which shows that three-dimensional disturbances assume major importance at Mach numbers above two. (Previous theories have only considered two-dimensional disturbances).

At the other end of the Reynolds-number scale are the flight results obtained by Fischer and Norris[34], again with a V-2–type missile but this time there were various surface discontinuities present, the measurements were taken during a climb from 30,000 ft to 100,000 ft and there were no records of pitch or yaw (*see* section 7.4 below for possible effects of the latter). Once again transition was determined from the skin-temperature measurements.

Of the tunnel-test results it should be noted that the high-transition Reynolds numbers obtained by Czarnecki and Sinclair[50] were on the RM-10 which is a body with a favourable pressure gradient along the majority of its length.

Despite the wide variation shown in Fig. 26 of transition Reynolds number under zero heat conditions (Re_{T0}) it is remarkable that all the results for cooling ($T_w/T_{w0} < 1$) lie on lines of approximately the same slope. This is illustrated further by Fig. 27 where the variation in Re_{T0} is eliminated by plotting the Re_T/Re_{T0} against T_w/T_{w0}, using the individual values of Re_{T0} shown in Fig. 26. Fig. 27 shows that on this basis all the results for cooling can be fitted by a single line. This is in qualitative agreement with the results of Fig. 25 for critical Reynolds number, since the experimental results are mainly in the range $1 \cdot 5 < M_1 < 2 \cdot 5$.

This does not necessarily mean that for all the cases considered in Figs. 26 and 27, transition is caused by the amplification of Tollmien-Schlichting waves, because Gadd[53] has shown that cooling can delay the separation of a laminar boundary layer subjected to an adverse pressure gradient. Hence it is possible that cooling may also delay transition which results from turbulence in the stream outside the boundary layer (Taylor's assumption, section 7.1.1. above).

Whatever the mechanism causing transition, further experimental evidence is required to bridge the gap between the tunnel and the flight results in Fig. 27.

On the heating side of the graph in Fig. 27 ($T_w/T_{w0} > 1$) the variation of Re_T/Re_{T0} is affected by the value of Re_{T0}. Here again, further experimental evidence is desirable.

Meanwhile it is suggested that the effect of cooling on transition may be estimated from the curve in Fig. 27*, but there remains the difficulty of determining the value of Re_{T0} to be used. Some remarks on this follow in the next section.

7.2. *Transition Under Zero Heat-Transfer Conditions.*—The data of Fig. 26 are drawn from tests on a variety of models in a number of different wind tunnels, etc., and the individual models were not tested at a sufficient number of Mach numbers to make it possible to check any movements of transition with Mach number under zero heat-transfer conditions.

Better data for this purpose are given in Fig. 31. The results in this figure were obtained (or collected) by Love, Coletti and Bromm[59] and each set shows a definite decrease in zero heat-transfer transition Reynolds number Re_{T0} as the Mach number is increased. This agrees in direction with the theoretical trend shown in Fig. 24 for minimum critical Reynolds number.

Now earlier experience in supersonic wind tunnels sometimes indicated a trend towards an increase in Re_{T0} with increase in the operating Mach number (*e.g.*, the Royal Aircraft Establishment results[9,10] for a flat plate in Fig. 26). A possible explanation might be that in these cases the free-stream turbulence was the prime cause of transition. If so, then increasing the operating Mach number might be regarded as increasing the effective contraction ratio of the tunnel so that the free-stream turbulence level in the working section would be reduced with consequent

* (1956). Provided $1 \cdot 5 < M_1 < 2 \cdot 5$, since there is now evidence, from wind-tunnel tests, that cooling, as expressed by T_w/T_{w0}, is less effective in delaying transition at $M = 3$. This would agree with the trends shown in Fig. 25.

beneficial effect on transition (*cf.* Fig. 29). This is only offered as a tentative explanation and apart from assuming that the effective contraction ratio is determined by the ratio of the velocity in the working section to that in the settling chamber, it also assumes that no turbulence is generated in the nozzle.

However, these considerations and the differences between results from different tunnels shown in Figs. 31 and 26 makes it seem highly desirable to develop a technique for measuring turbulence levels in supersonic wind tunnels with an aim of producing correlations such as in Fig. 29.

Meanwhile Fig. 31 gives an idea of the zero heat-transfer transition Reynolds numbers which can be achieved in supersonic wind tunnels. In this respect it may be noted that the high values obtained on the RM-10 model at $M = 1 \cdot 62$ in the Langley 9-in. Tunnel were found to be very dependent on the surface finish of the model, whereas at $M = 2 \cdot 41$ the requirements were less stringent. Also, longitudinal pressure gradients are likely to affect the transition Reynolds number (*see* section 7.3 below).

As regards the flight case, even less can be said. If flight tests are made on particular models to test the effects of surface finish, etc., then it is obvious from Fig. 26 or 27 that surface temperatures must be measured so that the temperature effect can be eliminated. Similar considerations would apply to pitch and yaw (section 7.4 below).

Meanwhile the question of what zero heat-transfer transition position to use in performance calculations must remain a matter of individual choice. It may seem best to use the maximum values (3 million) found for a flat plate in incompressible flow (Fig. 29), if there is zero pressure gradient along the body. Alternatively it may be felt that if care is taken to obtain a smooth finish then transition Reynolds numbers of the order of 8 million may be feasible (*cf.* Sternberg's V-2 results[49] in Fig. 26).

7.3. *Effect of Pressure Gradients.*—7.3.1. *Theoretical considerations.*—Fig. 28 gives the results of calculations by Weil[52] on the stability of the laminar boundary layer subjected to pressure gradients under zero heat-transfer conditions. The stability analysis was similar to that of Lees[47] while the requisite steady-state velocity and temperature distributions were obtained by an extension of the Karman-Pohlhausen method used in incompressible flow.

The results are plotted in Fig. 28 as minimum critical Reynolds numbers based on momentum thickness of the boundary layer $Re_{\theta\,cr}$ against a pressure-gradient parameter:

$$\lambda = \frac{\left[\int_0^\delta \frac{\rho}{\rho_1}\,dy\right]^2}{\nu_1 \dfrac{T_1}{T_{w0}}} \frac{du_1}{dx},$$

which reduces in the case of incompressible flow to the well known parameter $\lambda = (\delta^2/\nu)(du_1/dx)$. Positive values of λ correspond to favourable pressure gradients and it is evident from Fig. 28 that these may have a very beneficial effect on transition at the lower supersonic Mach numbers. Theoretically, complete stability is obtained at $M = 1 \cdot 5$ if $\lambda = 4 \cdot 4$. On the other hand as the Mach number is increased (above $1 \cdot 5$) the effects of favourable pressure gradients decrease.

7.3.2. *Experimental results.*—No systematic experimental results are available to check the trends shown in Fig. 28, but it may be relevant that a zero heat-transfer transition Reynolds number of 11 million was obtained by Czarnecki and Sinclair[50] in a wind-tunnel test at $M = 1 \cdot 61$ on the RM-10, which had a favourable pressure gradient over most of its length (Fig. 26).

7.4. *Effect of Incidence.*—Sternberg[49] quotes the results of some wind-tunnel tests at $M = 3 \cdot 2$ on a cone of 20 degrees included angle, where at zero incidence, transition occurred at 3 million Reynolds number, but when the incidence was brought up to 3 degrees, transition on the upper surface moved forward to 1 million Reynolds number. (On the lower surface transition moved back beyond 3 million, but the exact value was not known).

This movement is understandable because of the cross-flows which develop when a body is at incidence to an air stream and a 3 to 1 change in transition Reynolds number for a change in incidence of 3 degrees is sufficiently serious to justify further work on the subject.

It also points to the necessity of measuring pitch and yaw when making flight tests concerning transition.

7.5. *Effect of Single Spanwise Roughness Elements.*—The only available evidence concerning the effects of surface condition on transition position under zero heat-transfer conditions at supersonic speeds is for single spanwise roughness elements and is shown in Fig. 30, where it is compared with an empirical curve given by Gazley[4] for the incompressible-flow case.

The symbols are explained by the inset sketch and it is notable that the position of the roughness element does not appear in Gazley's correlation of the incompressible-flow results*. *See* Ref. 4 for further details.

The experimental results shown in Fig. 30 are:

(*a*) a result obtained by Scherrer[12] for an $0 \cdot 001$-in. diameter wire located $0 \cdot 8$ in. from the tip of a cone of 20-deg included angle (transition occurred at the wire)

(*b*) some unpublished results obtained at the R.A.E. for screw-thread–type roughness elements on a cone of 10-deg included angle. In this case transition occurred downstream of the roughness elements.

Both cases were for zero heat-transfer conditions.

It is of interest that the results are of the same order as found in incompressible flow, but further test results are needed to check the significance of this conclusion.

In his review[4] Gazley includes evidence from other sources which would seem to indicate that roughness elements are less effective in promoting transition in supersonic than in subsonic flow. This evidence is from:

(i) a V-2 firing by Fischer and Norris[34]

(ii) a cone in a firing range

(iii) a missile in a wind tunnel.

Now definitely in case (i), and probably in case (ii), the surface temperature was considerably less than its zero transfer value so that it is possible that the cooling effect discussed in section 7.1 may have delayed transition. This emphasises the need for further evidence and the necessity in all cases to measure the surface temperature.

* More recently, Dryden[60] has published a different correlation of the incompressible-flow results for single wires and flat strip elements (with transition occurring downstream of the roughness element), which gives a curve for the ratio of transition Reynolds number with roughness element present to that on the smooth plate as a function of the ratio of roughness height to boundary-layer displacement thickness (at the element).

8. *Brief Summary of Main Conclusions and Recommendations.*—The main purpose of this section is to group together the main conclusions which seem to be indicated by the survey. Greater detail will be found in the various sections to which references are given.

8.1. *Reliability of Formulae Available for Design Purposes.*—Reasonable confidence can be placed in the formulae for heat transfer with wholly laminar boundary layers (section 4.1) and with wholly turbulent boundary layers (section 4.2) at least up to local Mach numbers of 3*. It is possible that the effects of temperature gradients along the body can be catered for (section 5) and pressure-gradient effects are likely to be small for the shapes of body or wing used in supersonic flight.

Rough estimates can be made concerning the position of transition (section 7).

8.2. *Problems Requiring Further Work.*—8.2.1. *Concerning kinetic temperature rise.*—With laminar boundary layers there is need for flight tests giving local Mach numbers greater than two, to check the possible reduction in temperature recovery factor when the temperatures inside the boundary layer become high (section 3.1.3. and Fig. 5). Stagnation point temperatures are also required.

With turbulent boundary layers, data are required at Reynolds numbers greater than 10 million, for all Mach numbers. This is to check the variation with Reynolds number evidenced in Fig. 2 and section 3.1.1. Both wind-tunnel and flight tests would be suitable.

The effects of longitudinal temperature gradients require to be checked (section 5.2). This work would be done most easily in a wind tunnel.

8.2.2. *Concerning heat-transfer coefficients.*—The requirements are similar to those listed for kinetic temperature rise. There is need for flight-test data at all Reynolds and Mach numbers. There is also need for tests on the effects of temperature and pressure gradients which in the first place would best be met by systematic wind-tunnel tests (sections 5 and 6).

8.2.3. *Concerning transition.*—The whole subject requires further experimental evidence and care must be taken to isolate the various effects listed in section 7.

In flight tests it might be desirable to start by checking the effects of surface finish, although this by itself would also involve taking measurements of surface temperature, pitch and yaw so that true comparisons could be made between the individual tests.

On the wind-tunnel side there is need to develop the technique of turbulence measurement in supersonic flow. Meanwhile it is desirable when checking any transition movements, to test the same body in more than one wind tunnel.

The emphasis in all the above suggestions has been on the need for experimental data, but obviously there is also scope for further theoretical studies and preferably these should proceed in step with the test work.

---

* 1956. *See* footnote to section 4.2.1.1.

LIST OF SYMBOLS

Throughout this list the units of mass, length and time are slugs, feet and seconds. The unit of force is then the pound-weight or lb wt, and where it occurs it is denoted by lb. For checking purposes, lb wt $=$ slug ft/sec^2, and 1 slug $= 32 \cdot 17$ lb mass. The units of temperature and heat are deg C and C.H.U. (deg K $=$ deg C $+ 273$).

a		Local speed of sound (ft/sec)
c_f		Local skin friction coefficient
	$=$	$\tau_0/\frac{1}{2}\rho_1 u_1^2$
c_F		Mean skin-friction coefficient
	$=$	$\dfrac{\text{Total friction force on body}}{\frac{1}{2}\rho_1 u_1^2 \text{ (wetted area)}}$
c_p		Specific heat of air ($\simeq 7 \cdot 72$ for $T < 473$ deg K) (C.H.U./slug deg C)
g		Acceleration due to gravity (standard value $= 32 \cdot 17$) (ft/sec^2)
h		Newtonian heat-transfer coefficient {C.H.U./(ft^2 sec deg C)}
J		Mechanical equivalent of heat ($= 1400$) (ft lb/C.H.U.)
k		Thermal conductivity of air {C.H.U./(ft sec deg C)}
k_H		Local heat transfer coefficient
	$=$	$\dfrac{h}{\rho_1 u_1 c_p}$
$\bar{k}_H$		Mean heat-transfer coefficient
l		Total length of body (ft)
M		Mach number
	$=$	u/a
Pe		Peclet number
	$=$	$\dfrac{\rho c_p u x}{k}$
q		Heat-transfer rate per unit area (C.H.U./ft^2 sec)
$\bar{R}$		Gas constant (ft lb/slug deg K)
	$=$	3089
Re		Reynolds number
	$=$	$\dfrac{\rho u x}{\mu}$
Re_c		Critical Reynolds number for stability
Re_T		Transition Reynolds number
T		Temperature (deg K)
T_H		Total temperature
t		Time (sec)
u		Velocity (ft/sec)
x		Distance along body (ft)

Y_n		Coefficients used in assessing effects of temperature gradients
β		Temperature recovery factor
	$=$	$\dfrac{T_{w0} - T_1}{T_{H1} - T_1}$
δ		Thickness of boundary layer (ft)
μ		Viscosity of air (slug/ft sec)
ρ		Density of air (slug/ft^3)
	$=$	$2 \cdot 378 \times 10^{-3}$ at N.T.P.
σ		Prandtl number
	$=$	$\dfrac{c_p \mu}{k}$
τ_0		Local skin friction (lb/ft^2)

Subscripts

∞	Free stream ahead of body
1	Local stream outside boundary layer
w	At surface-temperature conditions
$w0$	At surface-temperature for zero heat transfer
i	Incompressible flow conditions

REFERENCES

No.	Author	Title, etc.
Bibliographies, Surveys, etc.		
1	H. A. Johnson and M. W. Rubesin ..	Aerodynamic heating and convective heat transfer—Summary of literature survey. Trans. A.S.M.E. Vol. 71. pp. 447 to 456. July, 1949.
2	—	Bibliography of aerodynamic heating and related subjects. U.S.A.F. Report 5633.
3	M. W. Rubesin, C. B. Rumsey and S. A. Varga	A summary of available knowledge concerning skin friction and heat transfer and its application to the design of high speed missiles. N.A.C.A. RM A51 J25a. NACA/TIB/2928. A.R.C. 15,024. November, 1951.
4	C. Gazley	Boundary-layer stability and transition in subsonic and supersonic flow: A review of available information with new data in the supersonic range. *J.Ae.Sci.*, Vol. 20. pp. 19 to 28. January, 1953.

No.	*Author*	*Title, etc.*
5	R. J. Monaghan	A review and assessment of various formulae for turbulent skin friction in compressible flow. C.P. 142. August, 1952.
	R. J. Monaghan	Some remarks on the choice and presentation of formulae for turbulent skin friction in compressible flow. R.A.E. Tech. Note Aero. 2246. May, 1953.
Properties of Air		
6	J. H. Keenan and J. Kaye	*Gas Tables.* Chapman and Hall, London, for John Wiley and Sons, New York. 1948.
Kinetic Temperature Rise		
7	H. M. Spivack	Experiments in the turbulent boundary layer of a supersonic flow. North American Aviation Report CM–615. TIB/P31952. January, 1950.
8	J. R. Stalder, M. W. Rubesin and T. Tendeland	A determination of the laminar transitional and turbulent boundary-layer temperature recovery factors on a flat plate in supersonic flow. N.A.C.A. Tech. Note 2077. June, 1950.
9	R. J. Monaghan and J. R. Cooke ..	The measurement of heat transfer and skin friction at supersonic speeds. Part III: Measurements of overall heat transfer and of the associated boundary layers on a flat plate at $M = 2\cdot43$. C.P. 139. December, 1951.
10	R. J. Monaghan and J. R. Cooke ..	The measurement of heat transfer and skin friction at supersonic speeds. Part IV: Tests on a flat plate at $M = 2\cdot82$. C.P. 140. June, 1952.
11	P. F. Brinich and N. S. Diaconis ..	Boundary layer development and skin friction at Mach number 3·05. N.A.C.A. Tech. Note 2742. July, 1952.
12	R. Scherrer	Comparison of theoretical and experimental heat-transfer characteristics of bodies of revolution at supersonic speeds. N.A.C.A. Report 1055. 1951.
13	W. F. Hilton	Wind-tunnel tests for temperature recovery factors at supersonic velocities. *J.Ae.Sci.* Vol. 18. pp. 97 to 100. February, 1951.
14	H. A. Stine and R. Scherrer	Experimental investigation of the turbulent–boundary-layer temperature recovery factor on bodies of revolution at Mach numbers from 2·0 to 3·8. N.A.C.A. Tech. Note 2664. March, 1952.
15	B. des Clers and J. Sternberg	On boundary-layer temperature recovery factors. Readers Forum. *J.Ae.Sci.* Vol. 19. pp. 645, 646. September, 1952.
16	G. R. Eber	Recent investigation of temperature recovery and heat transmission on cones and cylinders in axial flow in the N.O.L. Aeroballistics Wind Tunnel. *J.Ae.Sci.* Vol. 19. pp. 1 to 6. January, 1952.
17	F. V. Davies	Boundary-layer measurements on 10 deg and 20 deg cones at $M = 2\cdot45$ and zero heat transfer. C.P. 264. November, 1954.
18	L. T. Chauvin and C. A. de Moraes ..	Correlation of supersonic convective heat transfer coefficients from measurements of the skin temperature of a parabolic body of revolution. (N.A.C.A. RM–10). N.A.C.A. RM. L51A18. NACA/TIB/2534. March, 1951.
19	W. B. Fallis	Heat transfer in the transitional and turbulent boundary layers of a flat plate at supersonic speeds. Univ. of Toronto. Inst. of Aerophysics Report 19. P38593. May, 1952.
20	L. Crocco	Laminar boundary layer in gases (Lo strato limite laminare nei gas). Monografie scientifiche di aeronautica No. 3. A.C.A. Rome. December, 1946. R.A.E. Translation 218. A.R.C. 11,453. December, 1947.

No.	Author	Title, etc.
21	Edited by S. Goldstein	*Modern Developments in Fluid Dynamics.* Clarendon Press, Oxford. 1938.
22	H. B. Squire	Heat-transfer calculation for aerofoils. R. & M. 1986. November, 1942.
23	E. B. Klunker and F. E. McLean ..	Laminar friction and heat transfer at Mach numbers from 1 to 10. N.A.C.A. Tech. Note 2499. October, 1951.
24	G. B. W. Young and E. Janssen ..	The compressible boundary layer. *J.Ae.Sci.* Vol. 19. p. 229. April, 1952.
25	M. Tucker and S. H. Maslen	Turbulent–boundary-layer temperature recovery factors in two dimensional supersonic flow. N.A.C.A. Tech. Note 2296. February, 1951.
26	E. Eckert and W. Weise	The temperature of unheated bodies in a high-speed gas stream. N.A.C.A. Tech. Memo. 1000. February, 1941.
27	E. Eckert and W. Weise	Measurement of temperature distribution on the surface of unheated bodies in high velocity flow. Forschung auf dem Gebiete des Ingenieurwesens. Vol. 13. pp. 246 to 254. 1942.
28	G. R. Eber	Experimental research on friction temperature and heat transfer for simple bodies at supersonic velocities. Peenemünde Archiv 66/57. 1941.
29	L. Kovasznay	The hot-wire anemometer in supersonic flow. *J.Ae.Sci.* Vol. 17. pp. 565 to 572. September, 1950.
30	T. Nonweiler	Surface conduction of heat transferred from a boundary layer. College of Aeronautics Report 59. A.R.C. 15,058. May, 1952.

Heat Transfer

See Refs. 9, 10, 12, 16, 18, 19 to 24, 28 to 30, also.

No.	Author	Title, etc.
31	A. D. Young	Skin friction in the laminar boundary layer in compressible flow. College of Aeronautics Report 20. A.R.C. 11,936. July, 1948.
32	R. J. Monaghan	An approximate solution of the compressible laminar boundary layer on a flat plate. R. & M. 2760. November, 1949.
33	W. Mangler	Compressible boundary layers on bodies of revolution. M.A.P. Völkenrode Ref. MAP–VG83–47T. March, 1946. Also *see* R.A.E. Library Translation 417. December, 1952.
34	W. W. Fischer and R. H. Norris ..	Supersonic convective heat transfer correlation from skin temperature measurements on a V–2 rocket in flight. Trans. A.S.M.E. Vol. 1. pp. 457 to 469. July, 1949.
35	R. J. Monaghan and J. E. Johnson ..	The measurement of heat transfer and skin friction at supersonic speeds. Part II. Boundary-layer measurements on a flat plate at $M = 2 \cdot 5$ and zero heat transfer. C.P. 64. December, 1949.
36	W. H. McAdams	Heat transmission. McGraw Hill. 1942.
37	C. du P. Donaldson	Heat transfer and skin friction for turbulent boundary layers on heated or cooled surfaces at high speeds. N.A.C.A. RM L52 H04. NACA/TIB/3395. October, 1952.
38	E. Brun	La convection forcée de la chaleur aux grandes vitesses et aux températures élevées. Journal de Recherches du C.N.R.S. No. 18. p. 197. March, 1952.
39	W. Tessin and M. Jakob	Influence of unheated starting sections on the heat transfer from a cylinder to gas streams parallel to the axis. A.S.M.E. Preprint Paper 52–F–21. September, 1952.

No.	Author	Title, etc.
40	M. W. Rubesin	The effect of an arbitrary surface-temperature variation along a flat plate on the convective heat transfer in an incompressible turbulent boundary layer. N.A.C.A. Tech. Note. 2345. April, 1951.
41	E. G. Slack	Experimental investigation of heat transfer through laminar and turbulent boundary layers on a cooled flat plat at a Mach number of 2·4. N.A.C.A. Tech. Note 2686. April, 1952.
42	M. J. Lighthill	Contributions to the theory of heat transfer through a laminar boundary layer. *Proc. Roy. Soc.* A 1070. pp. 359 to 377. August, 1950.
43	D. R. Chapman and M. W. Rubesin ..	Temperature and velocity profiles in the compressible laminar boundary layer with arbitrary distribution of surface temperature. *J.Ae.Sci.* 16, pp. 547 to 565. September, 1949.
44	A. E. Bryson and R. H. Edwards ..	The effect of nonuniform surface temperature on the transient aerodynamic heating of thin skinned bodies. *J.Ae.Sci.* 19. pp. 471 to 475. July, 1952.
45	F. V. Davies and R. J. Monaghan ..	The estimation of skin temperatures attained in high speed flight. C.P. 123. February, 1952.
46	K. Stewartson	Correlated incompressible and compressible boundary layers. *Proc. Roy. Soc.* A 200. pp. 84 to 100. 1949.
Transition See Refs. 4, 9, 10, 12, 16, 34 also.		
47	L. Lees	The stability of the laminar boundary layer in a compressible fluid. N.A.C.A. Report 876. 1947.
48	E. R. Van Driest	Calculation of the stability of the laminar boundary layer in a compressible fluid on a flat plate with heat transfer. *J.Ae.Sci.* 19. p. 801. December, 1952.
49	J. Sternberg	A free-flight investigation of the possibility of high Reynolds number supersonic laminar boundary layers. TIB/P38540. B.R.L. Report 821. June, 1952.
50	K. R. Czarnecki and A. R. Sinclair ..	Preliminary investigation of the effects of heat transfer on boundary layer transition on a parabolic body of revolution (NACA RM–10) at a Mach number of 1·61. N.A.C.A. Tech. Note 3165. April, 1954. N.A.C.A. Report 1240. 1955.
51	R. W. Higgins and C. C. Pappas ..	An experimental investigation of the effect of surface heating on boundary-layer transition on a flat plate in supersonic flow. N.A.C.A. Tech. Note 2351. April, 1951.
52	H. Weil	Effects of pressure gradients on stability and skin friction in laminar boundary layers in compressible fluids. *J.Ae.Sci.* 18. p. 311. May, 1951.
53	G. E. Gadd	The numerical integration of the laminar compressible boundary-layer equations with special reference to the position of separation when the wall is cooled. A.R.C. 15,101. August, 1952.
54	G. E. Gadd, D. W. Holder and J. D. Regan	The interaction of an oblique shock wave with the boundary layer on a flat plate. Part II. Interim note on the results for $M = 1 \cdot 5$, 2, 3 and 4. A.R.C. 15,591. January, 1953.

Additional references mainly received since the completion of the main text:

Recovery Factor

No.	Author	Title, etc.
55	E. B. Klunker and F. E. McLean ..	Effect of thermal properties on laminar boundary-layer characteristics. N.A.C.A. Tech. Note 2916. March, 1953.
56	M. Bloom	Remarks on thermal characteristics of boundary layers. Readers Forum, *J.Ae. Sci.* 20. p. 363. May, 1953.

No.	Author	Title, etc.
Heat Transfer, etc.		
57	M. W. Rubesin	A modified Reynolds analogy for the compressible turbulent boundary layer on a flat plate. N.A.C.A. Tech. Note 2917. March, 1953.
58	L. E. Fraenkel	Calculations of the pressure distributions and boundary-layer development on a body of revolution with various parabolic afterbodies at supersonic speeds. R. & M. 2966. February, 1953.
Transition		
59	E. S. Love, D. E. Coletti and A. F. Bromm	Investigation of the variation with Reynolds number of the base wave and skin-friction drag of a parabolic body of revolution (NACA RM–10) at $M = 1\cdot62$, $1\cdot93$ and $2\cdot41$ in the Langley 9-in. Supersonic Tunnel. N.A.C.A./TIB/3432. N.A.C.A. RM L52H21. October, 1952. A.R.C. 15945.
60	H. L. Dryden	Review of published data on the effect of roughness on transition from laminar to turbulent flow. *J.Ae.Sci.* 20. pp. 477 to 482. July, 1953.
Additional references, added October, 1956.		
61	G. B. Schubauer and P. S. Klebanoff	Contributions on the mechanics of boundary-layer transition. N.A.C.A. Tech. Note 3489. September, 1955.
62	E. R. G. Eckert	Survey on heat transfer at high speeds. Wright Air Development Center, Technical Report 54–70. April, 1954.
63	R. J. Monaghan	On the behaviour of boundary layers at supersonic speeds. *Proceedings of the* 5*th Anglo-American Aeronautival Conference at Los Angeles.* June, 1955.
64	A. Seiff	Examination of the existing data on the heat transfer of turbulent boundary layers at supersonic speeds from the point of view of Reynolds analogy. N.A.C.A. Tech. Note 3284. August, 1954.
65	D. W. Dunn and C. C. Lin	On the stability of the laminar boundary layer in a compressible fluid. *J.Ae.Sci.* 22. p. 455. July, 1955.

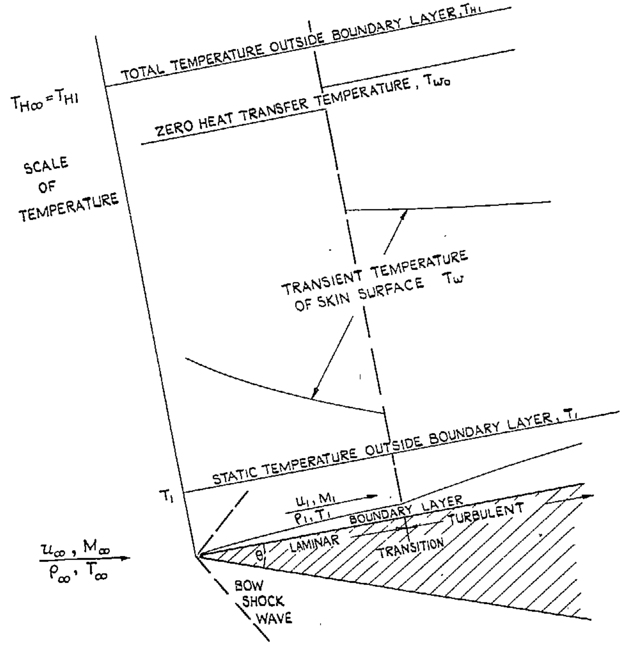

{TOTAL TEMPERATURE $T_{H1} = T_1 + \dfrac{u_1^2}{2 J c_p} = T_{H\infty}$,

RECOVERY FACTOR $\beta = \dfrac{T_{\omega o} - T_1}{T_{H1} - T_1}$,

HEAT TRANSFER COEFFICIENT IS BASED ON TEMPERATURE DIFFERENCE $(T_{\omega o} - T_\omega)$ }

FIG. 1. Conditions affecting convective heat transfer to a body in high-speed flight.

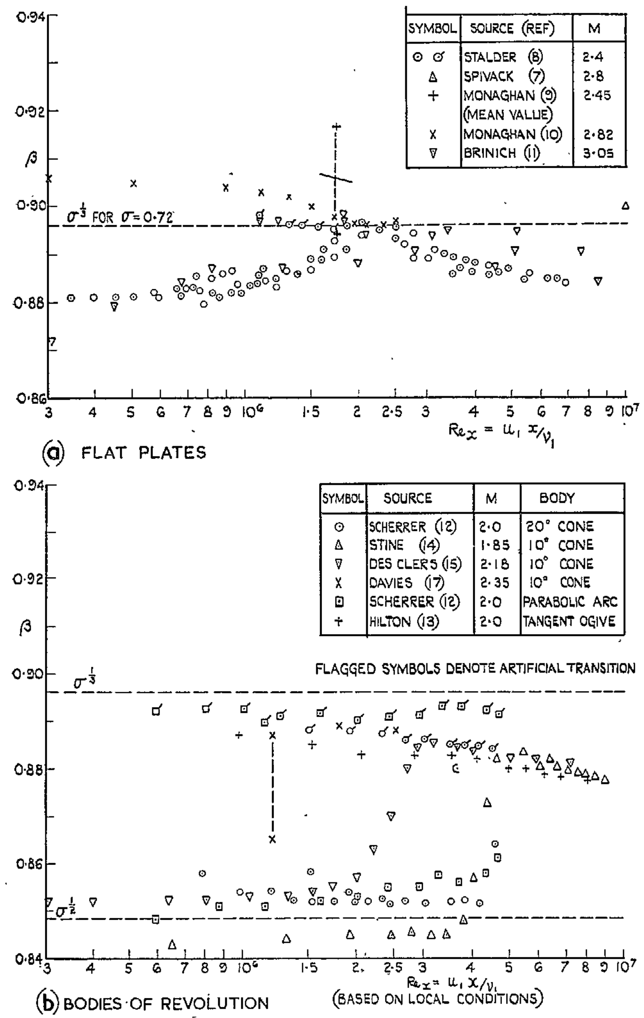

FIGS. 2a and 2b. Temperature recovery factors determined in continuous-flow wind tunnels.

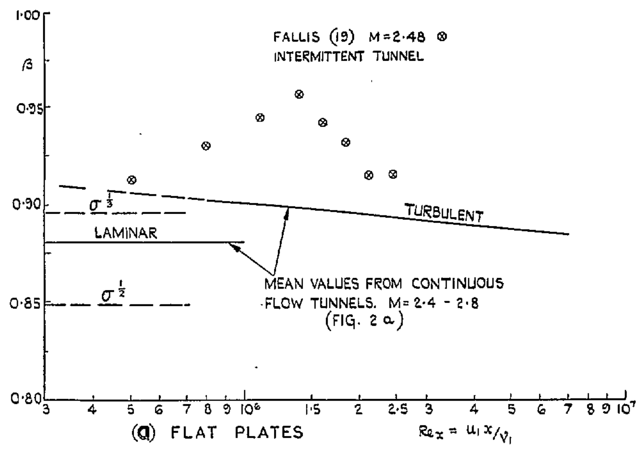

INTERMITTENT TUNNELS			
SYMBOL	SOURCE	M	BODY
⊙	EBER (16)	2·9	40° CONE-CYLINDER
⊡	EBER (16)	4·2	40° CONE-CYLINDER
∇	STINE (14)	3·2	40° CONE-CYLINDER
Δ	STINE (14)	3·7	40° CONE-CYLINDER
x	STINE (14)	3·7	10° CONE

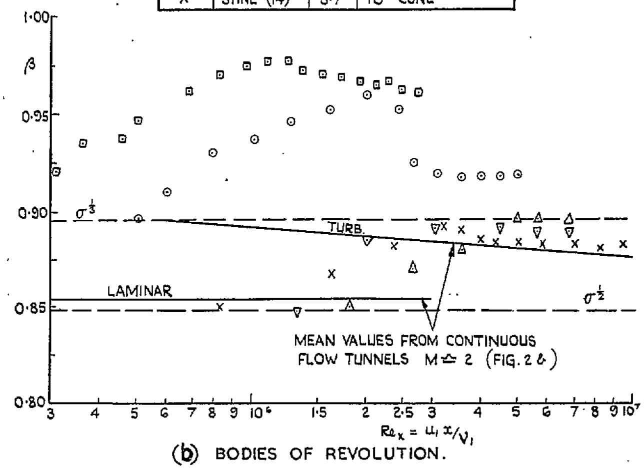

FIGS. 3a and 3b. Comparison of temperature recovery factors from continuous-flow and intermittent-flow wind tunnels.

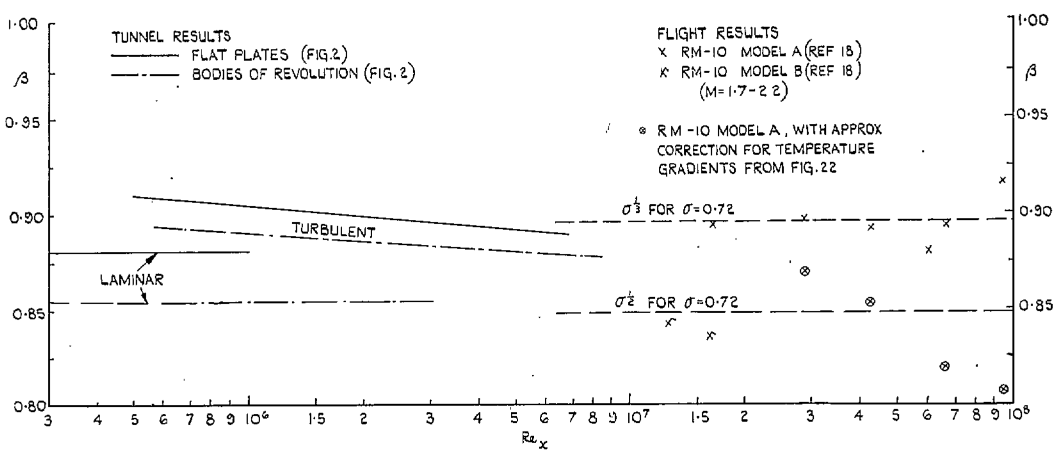

FIG. 4. Comparison of wind-tunnel and flight results for temperature recovery factor.

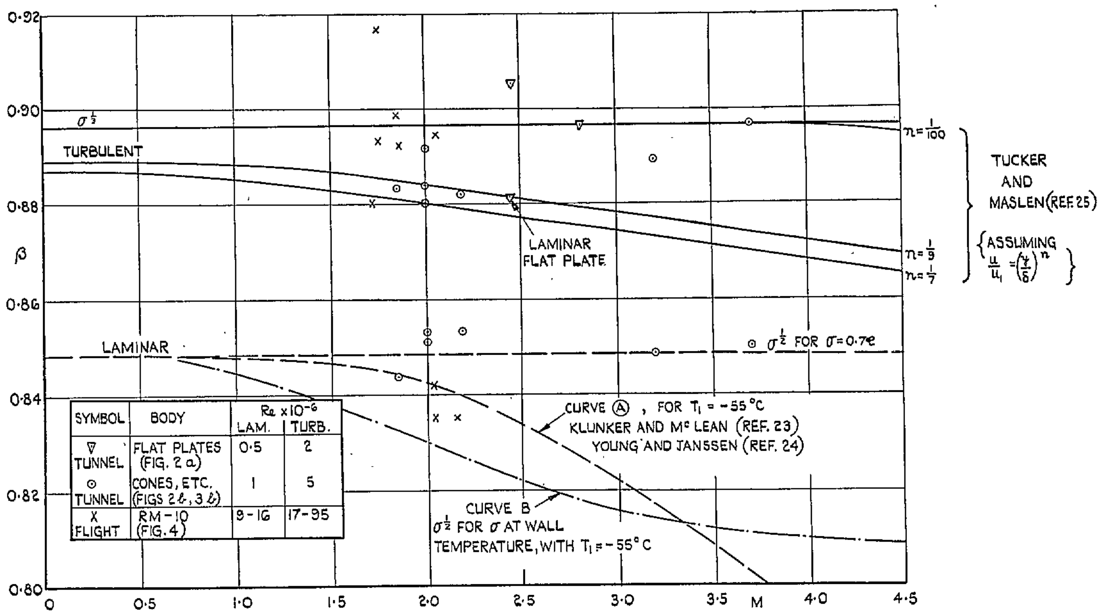

FIG. 5. Effect of Mach number on temperature recovery factor.

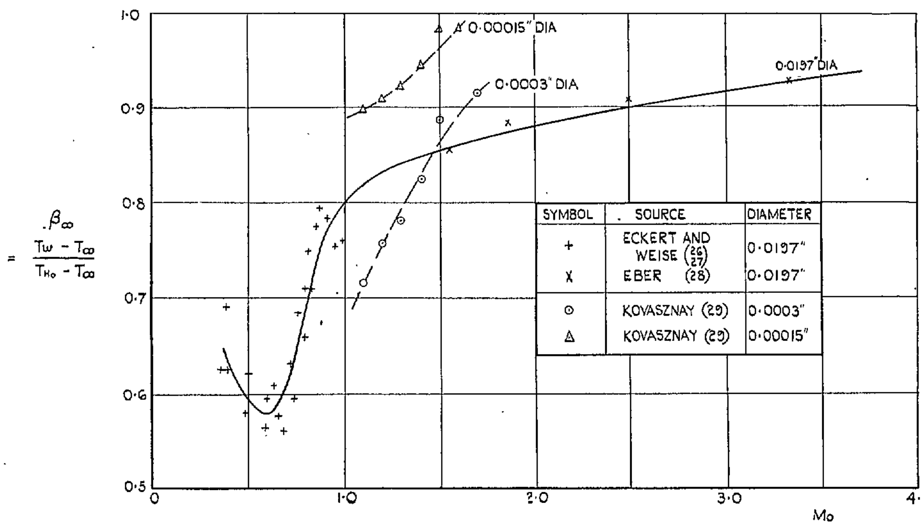

FIG. 6. Overall temperature recovery factor for a wire stretched across an air stream.

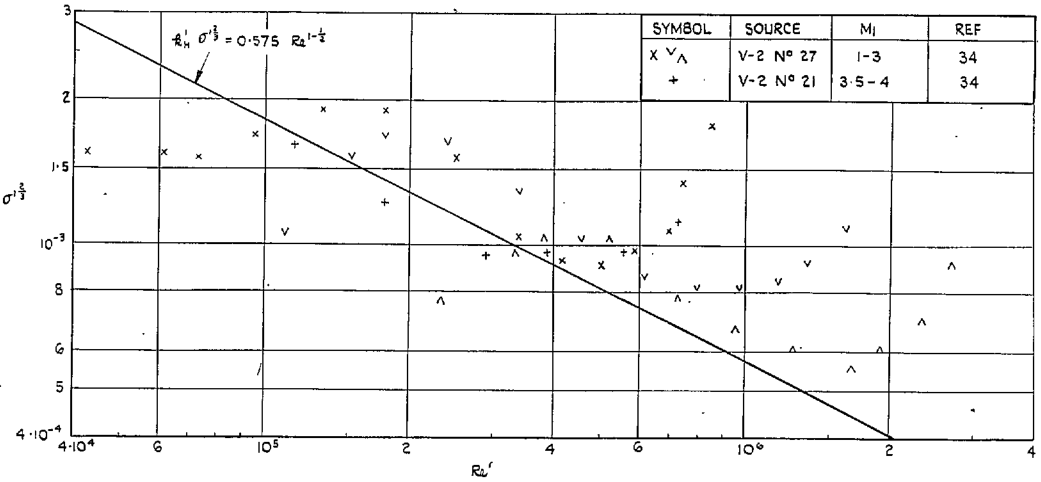

FIG. 7. Local heat-transfer coefficients for cones. Laminar boundary layer (Physical properties based on intermediate temperature T').

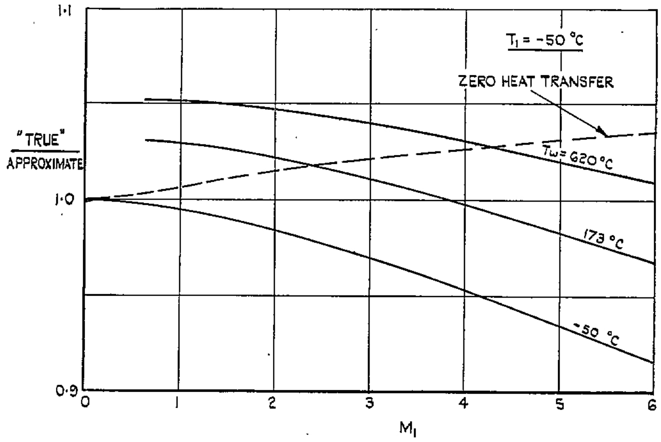

FIG. 8. Errors introduced by using approximate formula $k_{Hw}\sigma_w^{2/3} = CRe_w^{-1/2}$ in place of the 'true' formula $k_H'\sigma'^{2/3} = C(Re')^{-1/2}$ (*See* section 4.1 for heat transfer with a laminar boundary layer).

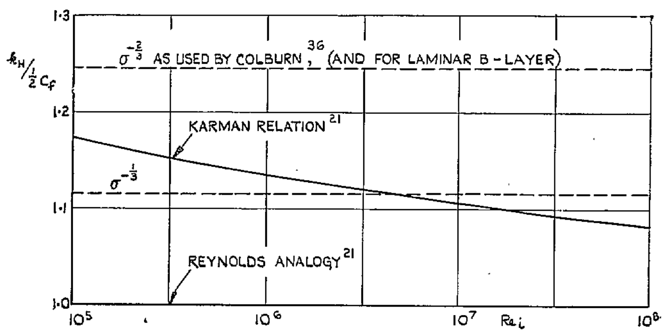

FIG. 9. Theoretical relations between turbulent heat transfer and skin friction for $\sigma = 0\cdot72$. Incompressible flow.

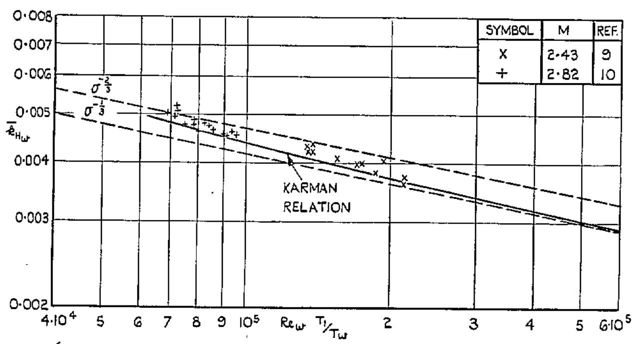

($\bar{k}_{H_w}$ = MEAN HEAT TRANSFER COEFFICIENT

PHYSICAL PROPERTIES OF AIR EVALUATED AT SURFACE TEMPERATURE $T_w = 373\ °K$.

THEORETICAL CURVES BASED ON MEAN SKIN FRICTION EQUATION $C_{F_w} = 0\cdot074 \left(Re_w \frac{T_1}{T_w}\right)^{-\frac{1}{5}}$ AND VALUES OF $k_H / \frac{1}{2} C_F$ FROM FIG.9 ABOVE.)

FIG. 10. Experimental results for turbulent heat transfer from a flat plate in compressible flow.

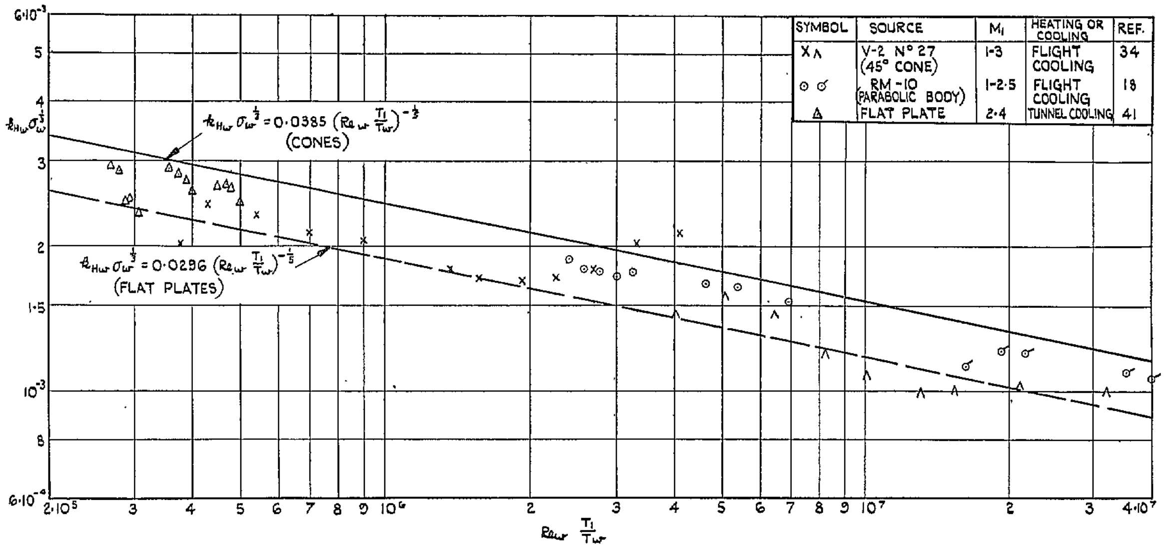

FIG. 11. Local heat-transfer coefficients. Turbulent boundary layer ($\sigma^{1/3}$ basis).

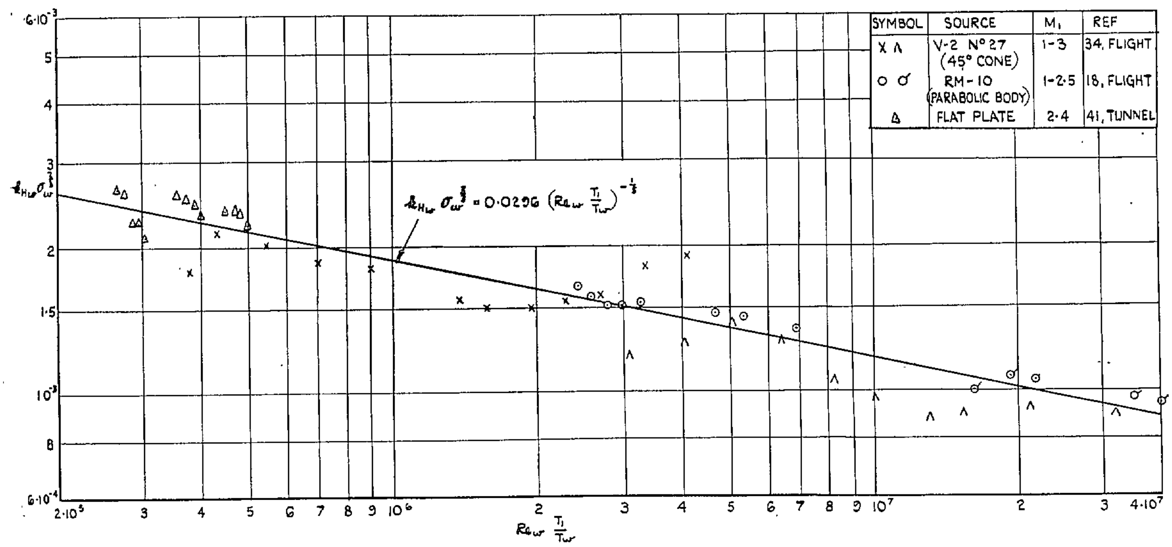

FIG. 12. Local heat-transfer coefficients. Turbulent boundary layer ($\sigma^{2/3}$ basis).

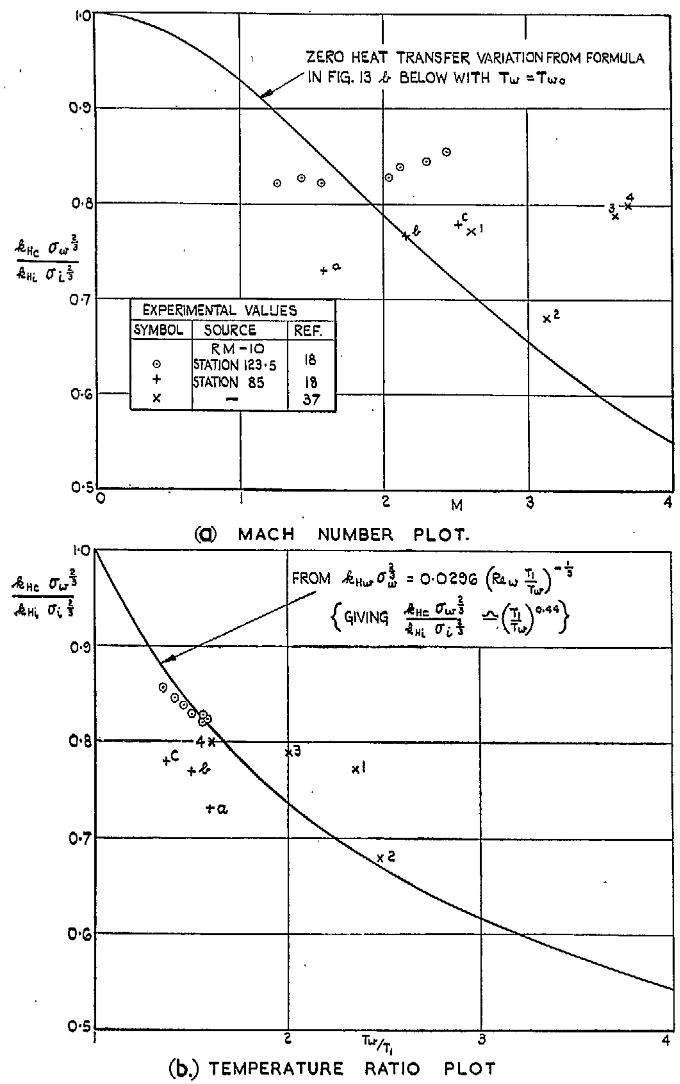

FIGS. 13a and 13b. Compressibility effect on local heat-transfer coefficient.

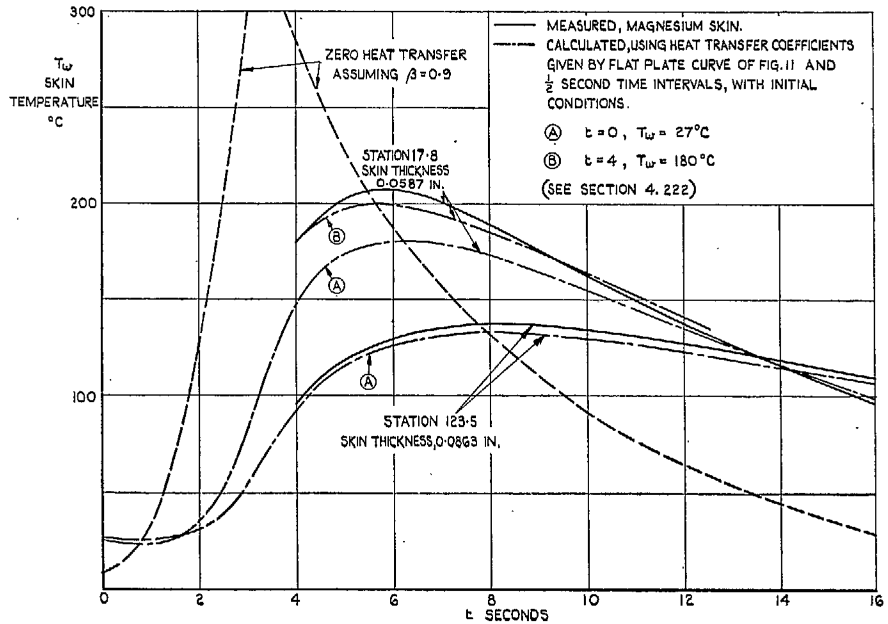

FIG. 14. Comparison between calculated and measured skin temperatures on RM–10 (Ref. 18).
(Showing effect of errors in heat-transfer coefficient).

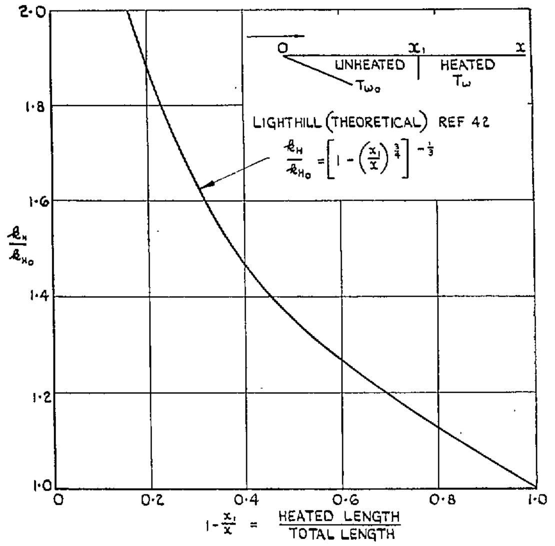

FIG. 15. Effect of unheated nose on local k_H. Theory for laminar boundary layer.

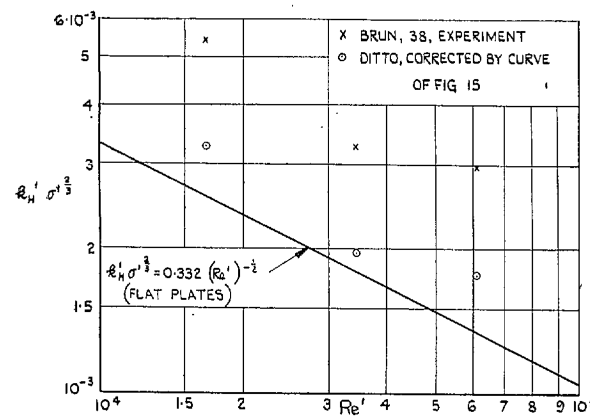

(BRUN'S RESULTS[38] ARE FOR $T_w \simeq 800°C$, $T_{H1} \simeq 25°C$ $1{\cdot}9 \leqslant M \leqslant 2{\cdot}9$ AND $1 - x_1/x = 0{\cdot}28$.)

FIG. 16. Effect of unheated nose on local k_H. Comparison of theory and experiment.

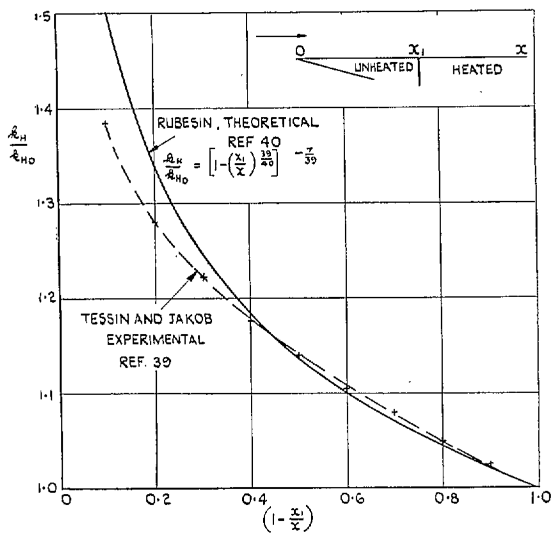

FIG. 17. Effect of unheated nose on local k_H. Incompressible flow. Turbulent boundary layer.

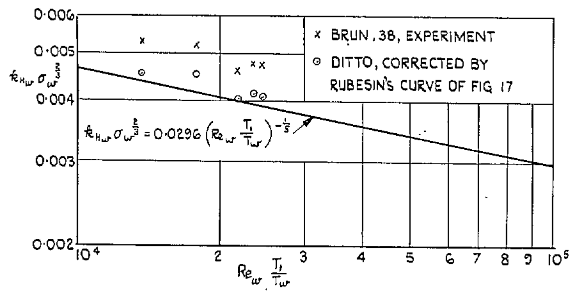

(BRUN'S RESULTS ARE FOR $T_w \simeq 750°C$, $T_1 \simeq 10°C$ $0{\cdot}35 \leqslant M \leqslant 0{\cdot}65$ AND $1 - x_1/x = 0{\cdot}42$.)

FIG. 18. Effect of unheated nose on local k_H. Compressible flow. Turbulent boundary layer.

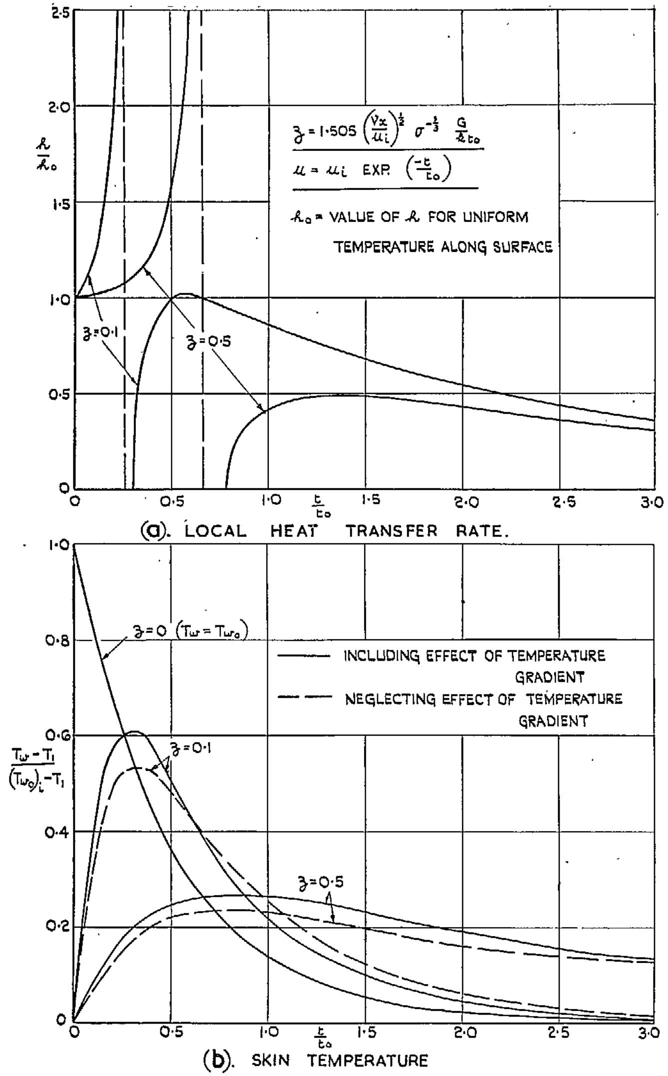

FIGS. 19a and 19b. Example of effects of non-uniform surface temperature on transient heating of thin-skinned body. Laminar boundary layer. (Taken from Ref. 44).

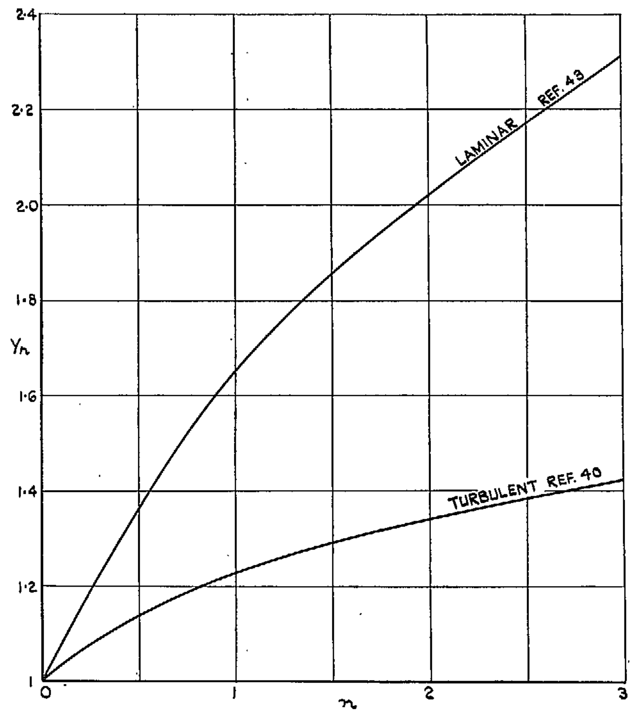

FIG. 20. Values of coefficients Y_n used in assessing effects of non-uniform surface temperature distributions on heat transfer (*See* section 5.2.1.).

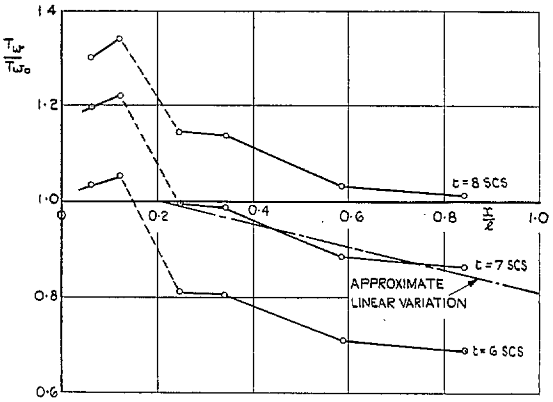

FIG. 21. RM-10[18]. Longitudinal temperature distributions near zero heat-transfer. Turbulent boundary layer.

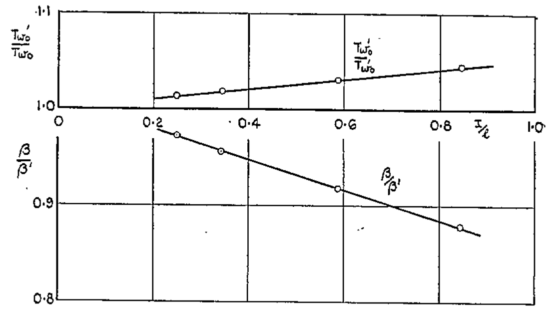

FIG. 22. RM-10[18]. Possible errors in recovery temperature and factor, assuming linear variation of temperature along body as in approximation of Fig. 21. (*See* section 5.2.1.1).

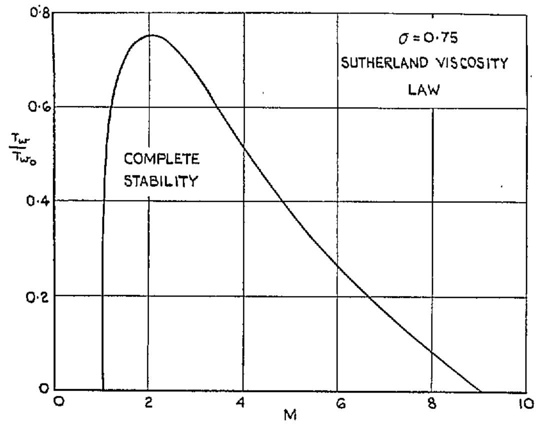

FIG. 23. Theoretical cooling requirements for complete stability of the laminar boundary layer (From Van Driest. Ref. 48).

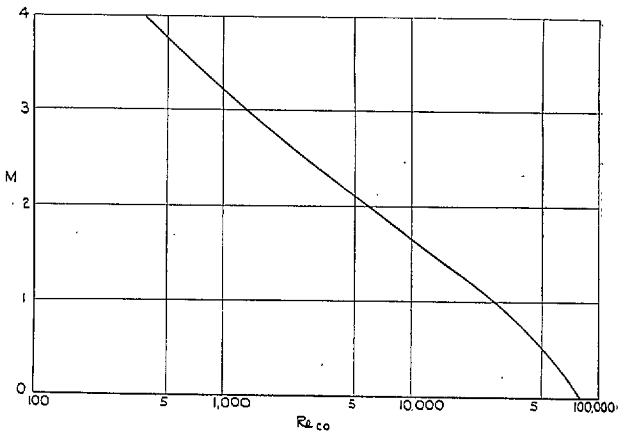

FIG. 24. Reduction of minimum critical Reynolds number with increasing Mach number under zero heat-transfer conditions (From Van Driest. Ref. 48).

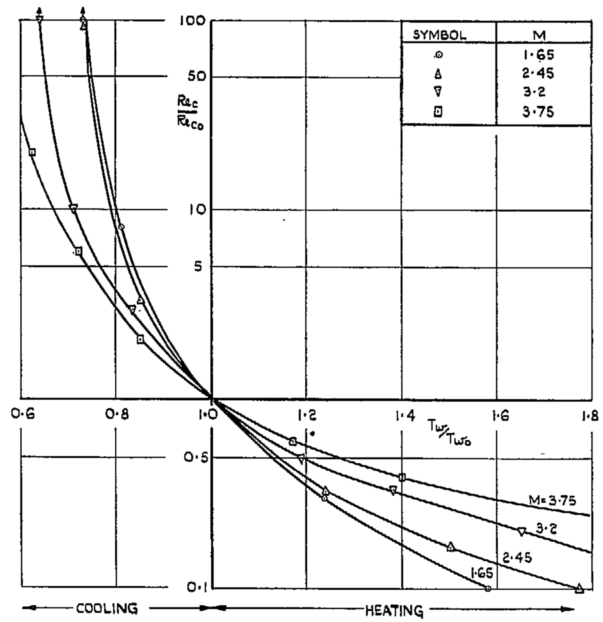

FIG. 25. Effect of heat transfer on minimum critical Reynolds number (From Van Driest, Ref. 48, for $\sigma = 0{\cdot}75$ and Sutherland viscosity law).

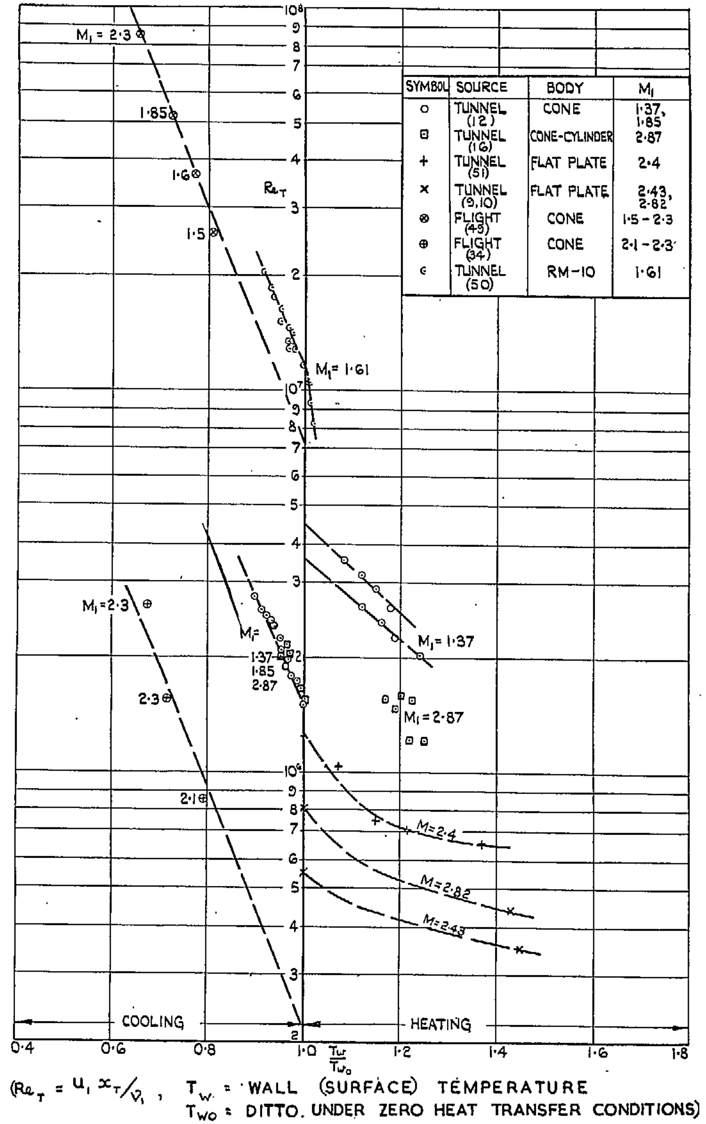

FIG. 26. Transition movements with heat transfer.

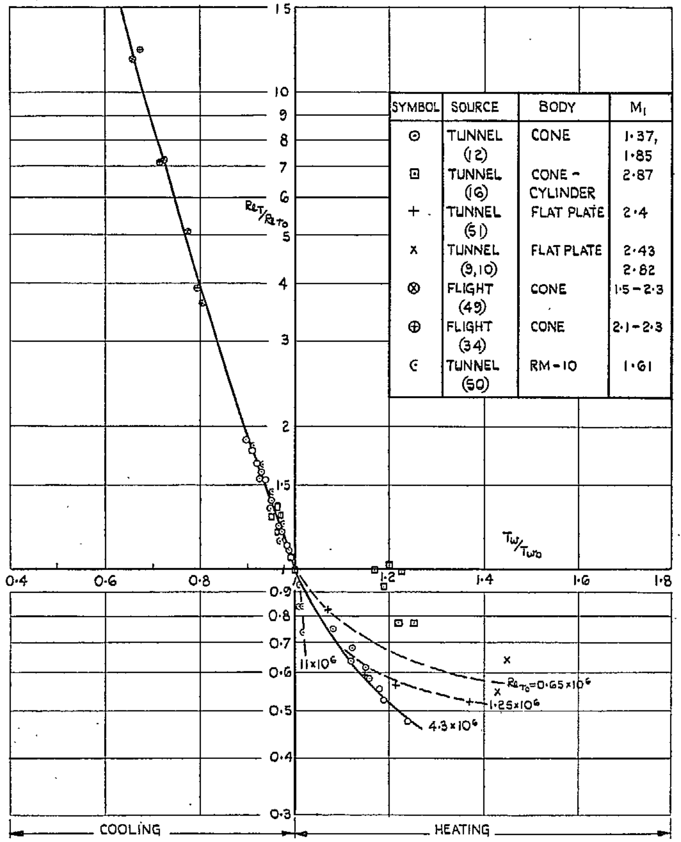

FIG. 27. Relative movement of transition with heat transfer.

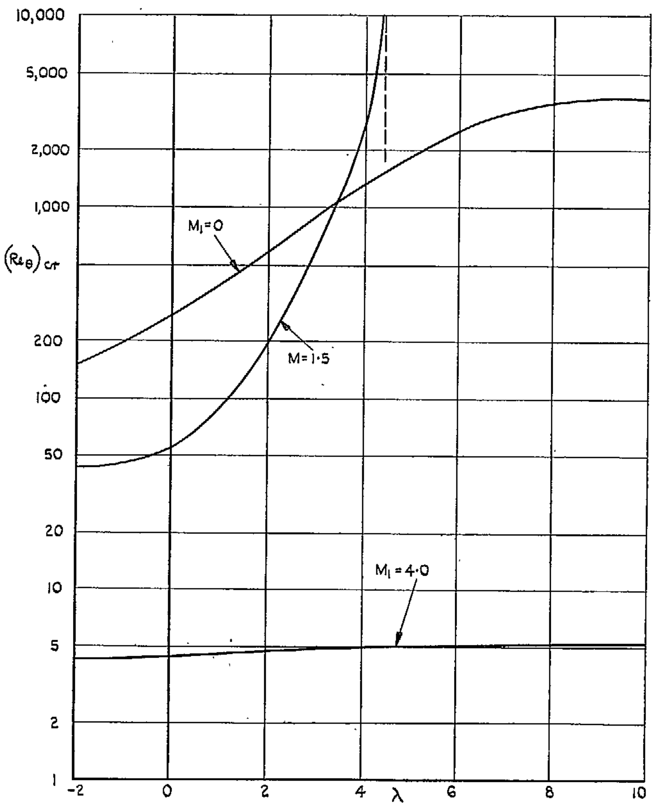

$$\lambda = \frac{\left[\int_0^\delta \frac{\rho}{\rho_1}\,dy\right]}{\nu_1 \frac{T_1}{T_{w0}}}\;\frac{du_1}{dx}\,, \quad Re_\theta = \frac{u_1 \theta}{\nu_1}$$

θ = MOMENTUM THICKNESS OF BOUNDARY LAYER

FIG. 28. Theoretical effect of pressure gradients on stability of laminar boundary layer (Results of H. Weil. Ref. 52).

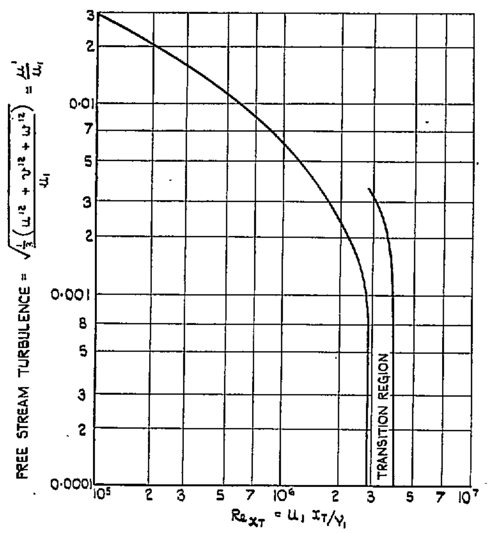

FIG. 29. Effect of free-stream turbulence on transition in incompressible flow over a flat plate (Curve as given by Gazley, Ref. 4).

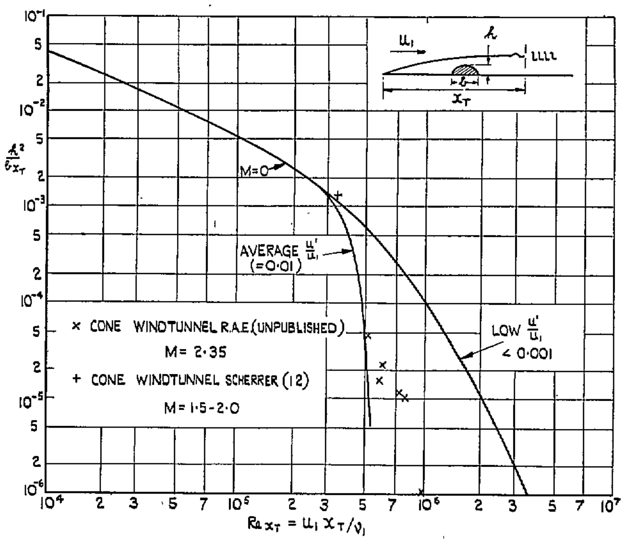

FIG. 30. Effect of spanwise roughness elements on transition (Zero heat-transfer conditions) (Correlation for $M = 0$ as given by Gazley, Ref. 4).

SYMBOL	BODY	TUNNEL	REF.
⊡	RM-10, 50" LONG	LANGLEY, 4 FT.	50, 59
⊙ ——	RM-10, 9" LONG	LANGLEY, 9 IN.	59
+ —·—	OGIVE - CYLINDER	LANGLEY, 9 IN.	59
× —··—	20° CONE-CYLINDER	N.O.L., 40 cm.	59
Λ ———	60° CONE-CYLINDER	N.O.L., 40 cm.	59

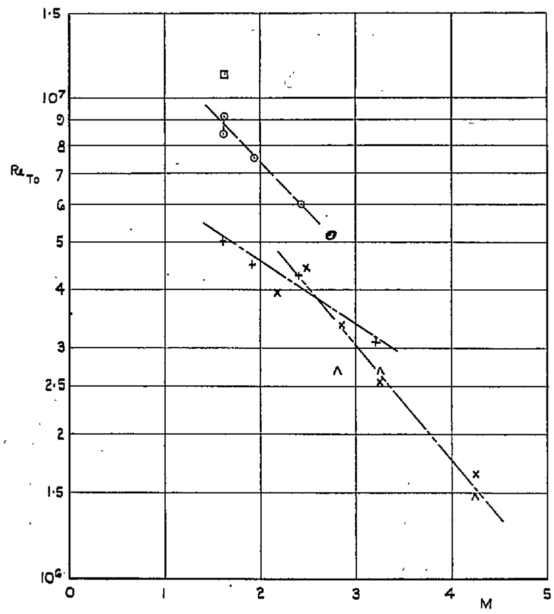

FIG. 31. Variations of transition Reynolds number with Mach under zero heat-transfer conditions. Wind-tunnel data as collected in Ref. 59.

(10766) Wt. 20/680 K7. 10/58 H.P.Co. 34-261

PRINTED IN GREAT BRITAIN

Publications of the Aeronautical Research Council

ANNUAL TECHNICAL REPORTS OF THE AERONAUTICAL RESEARCH COUNCIL (BOUND VOLUMES)—

1939 Vol. I. Aerodynamics General, Performance, Airscrews, Engines. 50*s.* (52*s.*)
Vol. II. Stability and Control, Flutter and Vibration, Instruments, Structures, Seaplanes, etc. 63*s.* (65*s.*)

1940 Aero and Hydrodynamics, Aerofoils, Airscrews, Engines, Flutter, Icing, Stability and Control, Structures, and a miscellaneous section. 50*s.* (52*s.*)

1941 Aero and Hydrodynamics, Aerofoils, Airscrews, Engines, Flutter, Stability and Control, Structures. 63*s.* (65*s.*)

1942 Vol. I. Aero and Hydrodynamics, Aerofoils, Airscrews, Engines. 75*s.* (77*s.*)
Vol. II. Noise, Parachutes, Stability and Control, Structures, Vibration, Wind Tunnels. 47*s.* 6*d.* (49*s.* 6*d.*)

1943 Vol. I. Aerodynamics, Aerofoils, Airscrews. 80*s.* (82*s.*)
Vol. II. Engines, Flutter, Materials, Parachutes, Performance, Stability and Control, Structures. 90*s.* (92*s.* 9*d.*)

1944 Vol. I. Aero and Hydrodynamics, Aerofoils, Aircraft, Airscrews, Controls. 84*s.* (86*s.* 6*d.*)
Vol. II. Flutter and Vibration, Materials, Miscellaneous, Navigation, Parachutes, Performance, Plates and Panels, Stability, Structures, Test Equipment, Wind Tunnels. 84*s.* (86*s.* 6*d.*)

1945 Vol. I. Aero and Hydrodynamics, Aerofoils. 130*s.* (132*s.* 9*d.*)
Vol. II. Aircraft, Airscrews, Controls. 130*s.* (132*s.* 9*d.*)
Vol. III. Flutter and Vibration, Instruments, Miscellaneous, Parachutes, Plates and Panels, Propulsion. 130*s.* (132*s.* 6*d.*)
Vol. IV. Stability, Structures, Wind Tunnels, Wind Tunnel Technique. 130*s.* (132*s.* 6*d.*)

ANNUAL REPORTS OF THE AERONAUTICAL RESEARCH COUNCIL—

1937 2*s.* (2*s.* 2*d.*) 1938 1*s.* 6*d.* (1*s.* 8*d.*) 1939–48 3*s.* (3*s.* 5*d.*)

INDEX TO ALL REPORTS AND MEMORANDA PUBLISHED IN THE ANNUAL TECHNICAL REPORTS, AND SEPARATELY—

April, 1950 . . . . . . R. & M. No. 2600 2*s.* 6*d.* (2*s.* 10*d.*)

AUTHOR INDEX TO ALL REPORTS AND MEMORANDA OF THE AERONAUTICAL RESEARCH COUNCIL—

1909–January, 1954 . . . R. & M. No. 2570 15*s.* (15*s.* 8*d.*)

INDEXES TO THE TECHNICAL REPORTS OF THE AERONAUTICAL RESEARCH COUNCIL—

December 1, 1936 — June 30, 1939	R. & M. No. 1850	1*s.* 3*d.* (1*s.* 5*d.*)
July 1, 1939 — June 30, 1945	R. & M. No. 1950	1*s.* (1*s.* 2*d.*)
July 1, 1945 — June 30, 1946	R. & M. No. 2050	1*s.* (1*s.* 2*d.*)
July 1, 1946 — December 31, 1946	R. & M. No. 2150	1*s.* 3*d.* (1*s.* 5*d.*)
January 1, 1947 — June 30, 1947	R. & M. No. 2250	1*s.* 3*d.* (1*s.* 5*d.*)

PUBLISHED REPORTS AND MEMORANDA OF THE AERONAUTICAL RESEARCH COUNCIL—

Between Nos. 2251–2349	R. & M. No. 2350	1*s.* 9*d.* (1*s.* 11*d.*)
Between Nos. 2351–2449	R. & M. No. 2450	2*s.* (2*s.* 2*d.*)
Between Nos. 2451–2549	R. & M. No. 2550	2*s.* 6*d.* (2*s.* 10*d.*)
Between Nos. 2551–2649	R. & M. No. 2650	2*s.* 6*d.* (2*s.* 10*d.*)
Between Nos. 2651–2749	R. & M. No. 2750	2*s.* 6*d.* (2*s.* 10*d.*)

Prices in brackets include postage

HER MAJESTY'S STATIONERY OFFICE

York House, Kingsway, London, W.C.2; 423 Oxford Street, London, W.1; 13a Castle Street, Edinburgh 2; 39 King Street, Manchester 2; 2 Edmund Street, Birmingham 3; 109 St. Mary Street, Cardiff; Tower Lane, Bristol 1; 80 Chichester Street, Belfast *or through any bookseller.*

S.O. Code No. 23–3033

R. & M. No. 303